NASA CONTRACTOR REPORT

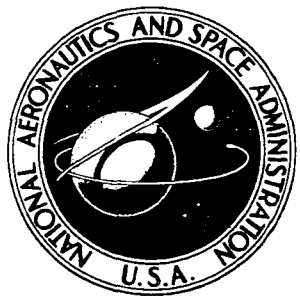

NASA CR-2413

NASA CR-2413

INVESTIGATION OF THE GROWTH OF GARNET FILMS BY LIQUID PHASE EPITAXY

by Jerry W. Moody, Roger W. Shaw, and Robert M. Sandfort

Prepared by
MONSANTO RESEARCH CORPORATION
St. Louis, Mo. 63166
for Langley Research Center

NATIONAL AERONAUTICS AND SPACE ADMINISTRATION • WASHINGTON, D. C. • JUNE 1974

1. Report No.	2. Government Accession No.	3. Recipient's Catalog No.
NASA CR-2413		

4. Title and Subtitle	5. Report Date
INVESTIGATION OF THE GROWTH OF GARNET FILMS BY LIQUID PHASE EPITAXY	June 1974
	6. Performing Organization Code
7. Author(s)	8. Performing Organization Report No.
Jerry W. Moody, Rodger W. Shaw, and Robert M. Sandfort	
9. Performing Organization Name and Address	10. Work Unit No.
	503-03-52
Monsanto Research Corp. N. Lindbergh Boulevard St. Louis, Missouri	11. Contract or Grant No.
	NAS1-11794
12. Sponsoring Agency Name and Address	13. Type of Report and Period Covered
National Aeronautics & Space Administration Washington, D.C. 20546	Contractor Report
	14. Sponsoring Agency Code

15. Supplementary Notes

FINAL REPORT

16. Abstract

Liquid phase expitaxy has been investigated to determine its applicability to fabricating magnetic rare earth garnet films for spacecraft data recording systems. Two mixed garnet systems were investigated in detail: (1) Gd-Y and (2) Eu-Yb-Y. All films were deposited on $Gd_3Ga_5O_{12}$ substrates.

The uniaxial anisotropy of the Gd-Y garnets is primarily stress-induced. These garnets are characterized by high-domain wall mobility, low coercivity and modest anisotropy. Characteristic length was found to be relatively sensitive to temperature.

The Eu-Yb-Y garnets exhibit acceptable mobilities, good temperature stability and reasonable quality factors. The uniaxial anisotropy of these garnets is primarily growth-induced. The system is well suited for compositional "tailoring" to optimize specific desirable properties.

Liquid phase epitaxy can be used to deposit $Gd_3Ga_5O_{12}$ spacing layers on magnetic garnet films and this arrangement possesses certain advantages over more conventional magnetic film-spacing layer combinations. However, it cannot be used if the magnetic film is to be ion implanted.

Considerations of the reproducibility and economics of the LPE process indicate that it is a commercially viable process. The relative simplicity of the apparatus and procedures and its adaptability combine to make it likely that LPE growth is the growth process of the future for magnetic bubble garnet films.

17. Key Words (Suggested by Author(s))	18. Distribution Statement
Liquid Phase Epitaxy Bubble Domain Garnet Thin Film	Unclassified - Unlimited STAR Category: 26

19. Security Classif. (of this report)	20. Security Classif. (of this page)	21. No. of Pages	22. Price*
Unclassified	Unclassified	64	$3.75

*For sale by the National Technical Information Service, Springfield, Virginia 22151

TABLE OF CONTENTS

TABLE OF CONTENTS (cont'd)

LIST OF FIGURES

LIST OF TABLES

INVESTIGATION OF THE GROWTH OF GARNET FILMS BY LIQUID PHASE EPITAXY

By Jerry W. Moody, Roger W. Shaw,
and Robert M. Sandfort
Monsanto Research Corporation

1. SUMMARY

The primary objective of this program was to investigate liquid phase epitaxy as a means to produce bubble-device quality films of magnetic rare-earth garnets. Two mixed garnet systems were investigated in detail: (1) Gd-Y and (2) Eu-Yb-Y. All films were deposited on $Gd_3Ga_5O_{12}$ substrates.

The uniaxial anisotropy of the Gd-Y garnets is primarily stress-induced. These garnets are characterized by high-domain wall mobility, low coercivity and modest anisotropy. Characteristic length was found to be relatively sensitive to temperature.

The Eu-Yb-Y garnets exhibit acceptable mobilities, good temperature stability and reasonable quality factors. The uniaxial anisotropy of these garnets is primarily growth-induced. The system is well suited for compositional "tailoring" to optimize specific desirable properties.

Liquid phase epitaxy can be used to deposit $Gd_3Ga_5O_{12}$ spacing layers on magnetic garnet films and this arrangement possesses certain advantages over more conventional magnetic film-spacing layer combinations. However, it cannot be used if the magnetic film is to be ion implanted.

Considerations of the reproducibility and economics of the LPE process indicate that it is a commercially viable process. The relative simplicity of the apparatus and procedures and its adaptability combine to make it likely that LPE growth is the growth process of the future for magnetic bubble garnet films.

2. INTRODUCTION

Objectives

The objectives of this program were specified in NASA Solicitation I-55-2610. Briefly, the overall objective was to evaluate liquid phase epitaxial (LPE) growth as a means to produce device

quality ferrimagnetic garnet films. The research was divided into a number of tasks and experiments which involved:

(1) Determination of growth conditions required to produce a magnetic film of a given composition.

(2) Investigation of the reproducibility and economics of the LPE process.

(3) Investigation of the relationship of film properties with film composition.

(4) Determination of the effects of post growth annealing on film properties.

(5) Evaluation of LPE growth as a manufacturing method.

(6) Investigation of the feasibility of depositing non-magnetic garnet films on ferrimagnetic films.

Two mixed garnet systems were investigated in detail. The $Gd_yY_{3-y}Fe_{5-x}Ga_xO_{12}$ system had been prepared elsewhere and provided a material system for the LPE process study. The $Eu_yYb_zY_{3-y-z}Fe_{5-x}Ga_xO_{12}$ system was chosen because it was expected to exhibit desirable q values, relatively high domain wall mobilities, good temperature stability and may have application in flight data recorder systems.

Experimental work on this project was initiated during June 1972. Brief, monthly letter reports have been issued during the course of the study. This detailed report constitutes the final report on the project.

Organization of the Report

Because of the wide scope and many objectives of the project, a chronological presentation of the work does not appear to be appropriate. For the sake of clarity and coherence, each subject is treated as an entity in the individual sections of this report. The mechanics of the LPE process are reviewed in Section 3. Characterization of films is discussed in Section 4. The properties of the $Gd_yY_{3-y}Fe_{5-x}Ga_xO_{12}$ and $Eu_yYb_zY_{3-y-z}Fe_{5-x}Ga_xO_{12}$ are presented in Section 5 and 6, respectively. Preparation of GGG spacing layers are described in Section 7. The reproducibility and economics of LPE growth are discussed in Section 8 and LPE and CVD techniques are compared in Section 9. Important conclusions and recommendations are summarized in Section 10. The appendix contains a description of substrate preparation techniques as well as characterization data on samples supplied to NASA.

3. LPE GROWTH OF GARNET FILMS

Background

The LPE growth of a rare earth magnetic garnet on a non-magnetic garnet substrate was first described by Linares, et al. (ref. 1,2). Later, Shick, (ref. 3) et al. utilized the process to grow films of uniaxial magnetic garnets suitable for bubble domain propagation. Levinstein, et al., (ref. 4) discovered the remarkable stability of supercooled solutions of garnet in $PbO-B_2O_3$ solvents and described a simple "dipping" method for the growth of epitaxial garnet films from isothermal solutions. Since then this relatively simple technique has been used extensively in the preparation of multicomponent uniaxial garnet films and was the method used in this work.

Most of the work has been done in PbO-based solvents, usually the $PbO-B_2O_3$ system. However, Linares (ref. 2) investigated other solvents including those based on BaO. Recently, the BaO-based solvent has been the subject of an intensive investigation by workers at Hewlett-Packard Laboratories (ref. 5). This solvent system exhibits several desirable features including low volatility, non-corrosiveness and low toxicity. However, the relatively high viscosity of the solvent and the attendant difficulties of drainage have been serious deterrents to its widespread use.

The solvent used in this work is that used by Shick, et al. (ref. 3) which consists of 94 mol % PbO and 6 mol % B_2O_3 (50:1 parts by weight).

Phase Relationships

The rare-earth magnetic garnets are incongruently saturating in the solvent chosen for this work as they are in all PbO-based solvents. The phase relationships in these systems require that the solutions contain an excess of Fe_2O_3 (over that required by the garnet formula) in order to maintain the system in the garnet stability region. It is convenient to discuss the phase relationships in terms of the molar compositional ratio:

$$R_1 = \frac{Fe_2O_3 + Ga_2O_3}{\Sigma R_2O_3}$$

where ΣR_2O_3 is the sum of the concentrations of all rare-earth oxides present. Orthoferrite precipitates from solutions where R_1 corresponds to the stoichiometric garnet ratio (5/3) whereas

magnetoplumbite is the stable phase for large R_1. It is difficult to determine the limits of the garnet field precisely because of the complexity of the solutions and their great tendency to supercool. However, from this study and other work done at Monsanto and from solution compositions given in the literature, the garnet stability region appears to range from R_1 equal to about 10 to about 30, the precise limits being dependent on the actual species of rare-earth ions present and their concentration in the melt. In general, the ratio defining the boundary between the orthoferrite and garnet fields decreases with increasing liquidus temperature. For example, an R_1 of about 12 is sufficient to place the solution in the garnet stability region for Eu-Yb-Y films grown at about 990°C, but an R_1 of about 16 is required for films of the same composition grown at about 910°C.

Solutions with compositions near the orthoferrite-garnet boundary are less stable with respect to supercooling than are solutions nearer the center of the garnet field; that is, the former are more likely to precipitate for any particular degree of supercooling. In addition, films grown from such solutions are likely to replicate the faceted core and growth striations of the substrate. Therefore, it is desirable to grow films from solution compositions well removed from the garnet/orthoferrite boundary. However, as R_1 is made large the yield of garnet from a particular solution decreases. Thus a compromise R_1 is selected which results in a stable supercooled solution and produces low defect films at good yields. A satisfactory R_1 is easily determined empirically by microscopic examination of films grown from solutions of various R_1.

Generally, an R_1 of 12 to 16 and a rare-earth oxide concentration of 0.55 to 0.65 mol % were used in this work. Such concentrations permitted film growth at temperatures ranging from about 920 to about 1000°C.

Liquidus temperature of these solutions is found to increase with total solute concentration ($R_2O_3 + Fe_2O_3 + Ga_2O_3$), increasing more rapidly with R_2O_3 than with $Fe_2O_3 + Ga_2O_3$. The liquidus temperature of a particular solution can be estimated by observing the temperature at which the last solids dissolve as a well-stirred solution is slowly heated. The liquidus temperature can be determined more accurately by plotting growth rate as a function of growth temperature for a series of films grown at various degrees of supercooling and extrapolating the curve to zero growth rate as is shown in Figure 1. Here the liquidus temperature, T_L, of the solution is estimated to be 953°C. Care must be taken to minimize loss of PbO by evaporation and to grow relatively thin films so that the solution composition does not change appreciably during the series of experiments.

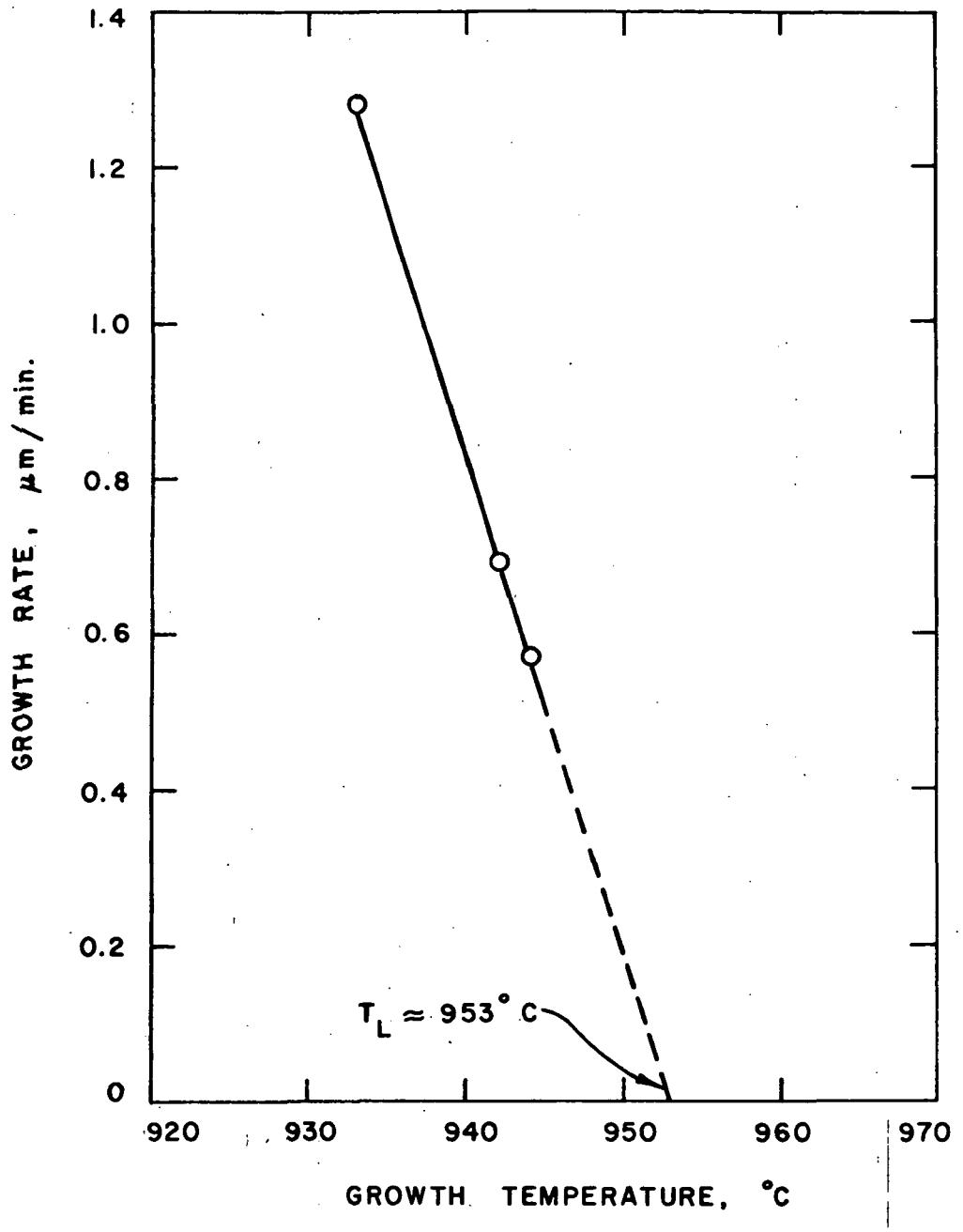

Figure 1. Estimation of Liquidus Temperature

Film Growth

In general, magnetic bubble films have been grown by the dipping method either statically or with rotation. In this work, all the Gd-Y films were grown statically from undisturbed melts and all Eu-Yb-Y films were grown with the substrate mounted horizontally and with axial rotation.

In undisturbed solutions, the growth rate depends on the concentration of solute and the degree of supercooling. For a particular solute concentration, growth rate is found to about double for each 10 degrees of supercooling. Although it is possible to achieve compositional uniformity by static growth it is exceedingly difficult to achieve the thickness uniformity required for device quality films.

Excellent thickness uniformity can be achieved by axial rotation of substrates mounted horizontally (ref. 6). The stirring of the solution by the rotating wafer tends to destroy any thermal or concentration gradients which might exist in the static solution. In addition, axial rotation permits improved control of the film growth processes by inducing a steady-state condition in the diffusion boundary layer at the film-solution interface.

It is believed that film growth with axial rotation has now been adopted by all growers of magnetic bubble materials. The mechanics and kinetics of the process have been the subject of recent studies (ref. 3). In this respect it is important to realize that, with axial rotation, film growth rate varies with rotation rate as well as solute concentration and supercooling. For a particular solution the growth rate is found to increase with the square root of the rotation rate as is shown in Figure 2. Here films were grown at rotation rates varying from 25 to 200 rpm at 8°C supercooling (ΔT) from a solution with a T_L of 953°C. Since the gallium distribution coefficient and the anisotropy of the films are growth rate dependent, rotation rate is an important parameter when establishing conditions for film growth. These factors are discussed in detail in Section 7 which deals with the reproducibility of the LPE process.

It has been found that the degree of thickness uniformity which is achieved at a particular rotation rate depends on the relative diameter of the substrate and crucible. In general, larger substrates require larger crucibles and higher rotation rates. For example, for substrates about 20mm in diameter and a crucible 45mm in diameter, a rotation rate of 200 rpm results in thickness uniformity of one percent. Higher rotation rates must be used for larger crucibles and the same size substrate. On the other hand, 200 rpm is sufficient to obtain excellent thickness uniformity for .25 mm diameter substrates in a 56 mm diameter crucible.

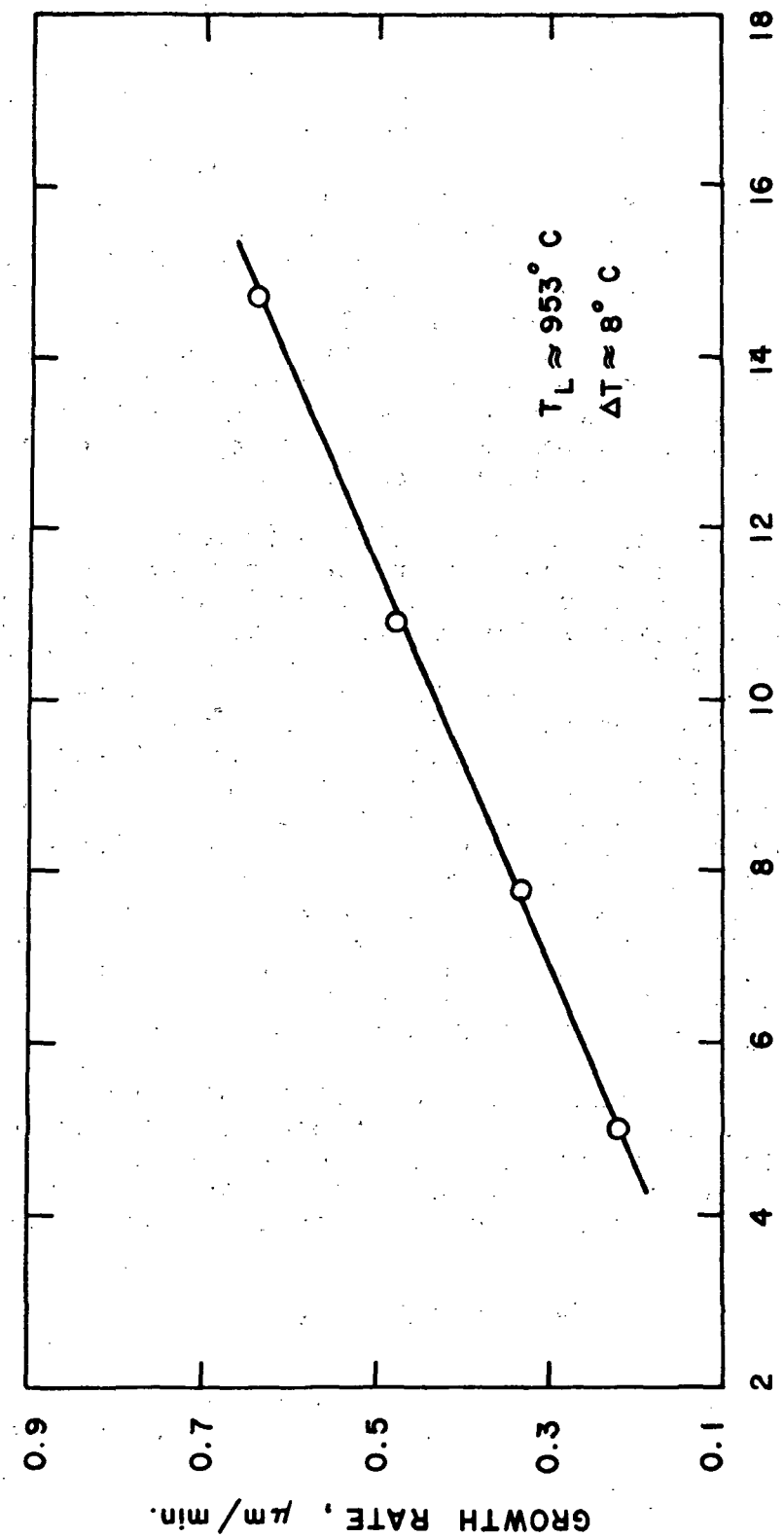

Figure 2. Dependence of Growth Rate on Rotation Rate

Apparatus and Experimental Procedures

Figure 3 is a schematic drawing of an LPE dipping station. The relatively simple apparatus consists of a Kanthal wound, resistance tube furnace mounted vertically. A close-fitting, heavy wall (1/4 in.) alumina tube is used to line the bore of the furnace. The liner serves primarily to protect the furnace windings from corrosive fumes. In some cases, the furnace bore has been lined with platinum and various platinum baffles were used to distribute the heat uniformly in the hot zone. However, equally satisfactory results have been obtained with the arrangement illustrated here. The platinum crucible containing the solution is supported on a firebrick pedestal slightly below the hottest zone of the furnace. The temperature is controlled with a Pt vs Pt - 10% Rh thermocouple placed against the alumina liner. A second Pt vs Pt - 10% Rh thermocouple is used to monitor the solution temperature. This thermocouple junction abuts the Pt crucible.

The substrate is mounted in a Pt wire holder which is attached to an alumina rod. The rod and substrate are moved in and out of the furnace by means of a crystal puller equipped with means for variable speed translational and rotational motion. Before the substrate is immersed in the solution it is held just above the melt surface for about 10 minutes to allow the substrate temperature to reach the solution temperature. The substrate is then dipped into the solution for a prescribed length of time during which film growth occurs. To ensure film thickness uniformity without axial rotation the substrate is tilted in its holder to conform approximately with an isotherm in the solution. If rotation is used the substrate is mounted horizontally. After the prescribed growth time, the substrate is raised from the melt. If rotation is used, it is stopped momentarily just as the substrate breaks the surface and, when the wafer is slightly above the melt surface, it is rotated at about 500 rpm to spin off any solution droplets which might adhere to the holder or wafer.

The oxides used in this work were of 99.99% purity. The oxides were weighed to four significant places and melted together in the Pt crucible. The solution was homogenized by stirring at about 1050°C, well above the liquidus temperature of the solutions used, for 2 to 4 hours before being cooled to growth temperatures.

4. CHARACTERIZATION

The majority of the methods employed in the characterization of the garnet films grown under this contract have been dealt with in detail in earlier reports (ref. 9,10,11). The following brief discussion is thus intended only to summarize these methods and present relevant detail where new techniques have been instituted since those reports were prepared.

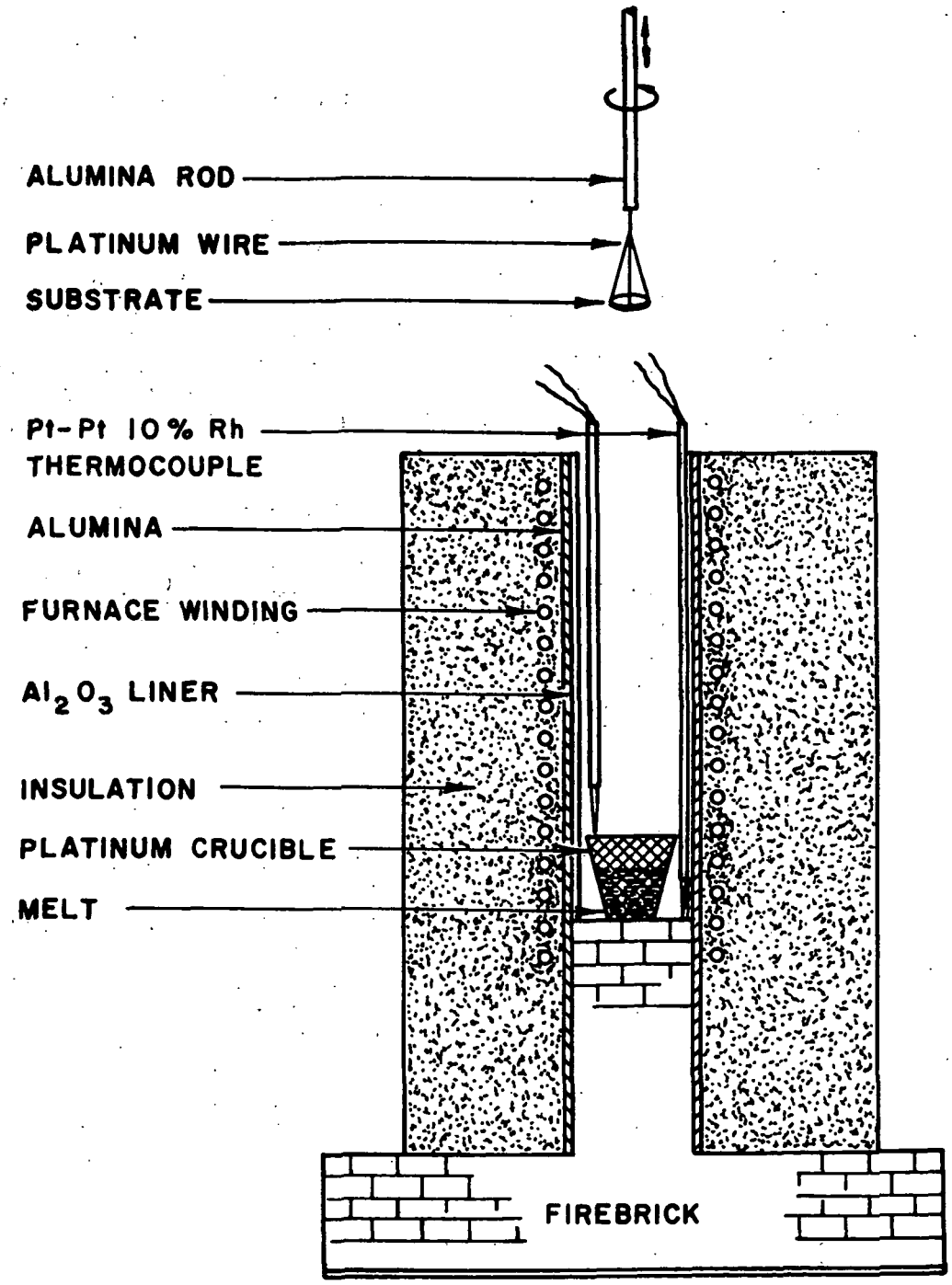

Figure 3. LPE Dipping Station

Film Thickness

The thickness of the magnetic garnet films has been measured using optical interference of reflected light (see ref. 10, p. 33). Thickness uniformity also has involved the use of optical interference, in this case in the form of a contour map caused by interference of monochromatic light reflected from the front and back of the film (see ref. 10, p. 40).

Defect Detection and Location

Defects which impede domain motion are readily observed using a polarizing microscope and an alternating bias field sufficient to cause most of the strip domains to move (see ref. 10, p. 49). Experience at Monsanto has indicated that this method, when properly employed, is sufficiently sensitive to detect all defects likely to cause difficulties in devices of present design.

Characteristic Length and Domain Dimensions

Where possible, domain dimensions have been measured on parallel strip domain patters in order to improve accuracy. This includes the determination of characteristic length from the film thickness and strip domain period (ref. 12,13,10, p. 58). Bubble domain diameters are routinely measured at the stability limits but such results are of more limited accuracy.

Saturation Magnetization and Magnetic Fields

The saturation magnetization was derived from the measurement of the highest bias field at which normal bubbles are stable (the collapse field) combined with a knowledge of the zero field strip domain width and the thickness. The theory required has been worked out by Thiele (ref. 14) and Fowlis and Copeland (ref. 15) with useful graphical results in several places (eq. ref. 10, p. 72). A calibrated bias coil mounted on the stage of a polarizing microscope served as source for most of the magnetic fields needed in the work. For situations in which the sample was inaccessable, as in a variable temperature stage, the saturation magnetization was usually derived from an optical hysteresis loop (ref. 13,10, p. 73).

Coercivity

A measure of sample coercivity results from determination of the polarized light intensity modulation resulting from several amplitudes of bias field modulation. The plot of light modulation vs field modulation amplitudes yields an approximately linear relationship which extrapolates, for zero light modulation, to a finite field amplitude -- the coercivity field (ref. 10, p. 118). This technique, while a worthwhile relative measure, usually yields values smaller than the half-width of the complete hysteresis loop and so has little absolute meaning. Experimentally, samples of coercivity greater than approximately 0.5 Oe show inferior characteristics in devices.

Anisotropy

The measurement of magnetic anisotropy field, H_A, by magneto-optical techniques, was just under development at the time of preparation of ref. 10. The recent papers of Shumate, et al. (ref. 15 and 16) place this measurement on a much better footing than it was at that time. In particular they form the basis for a technique proposed by Josephs (ref. 17) and now used almost exclusively in this laboratory. In this method a large field is applied in the plane of the film, rotating the magnetization into this plane. An alternating bias field normal to the film still yields a small optical modulation proportional to the susceptibility in the normal direction. For fields H greater than $H_A - 4\pi M_S$ this susceptibility is given by $\chi = M_S/(H + 4\pi M_S - H_A)$. Thus a plot of χ^{-1} (or the proportional inverse light modulation amplitude) vs H yields a linear relationship with an intercept at $\chi^{-1} = 0$ of $H = H_A - 4\pi M_S$. This linear relationship is quite consistently observed when the proper alignment of the sample has been established. The resulting values of H_A are accurate to roughly ±10%.

It should be noted that the method outlined in ref. 10, p. 113 -- the assignment of the low field shoulder as $H_A - 4\pi M_S$ -- is in error. This shoulder is, to within ∿10%, equal to H_A but its interpretation is not on as sound theoretical footing as is the method outlined above, so that the latter has been adopted as standard.

Domain Wall Dynamics

The basic measurement for domain wall mobility has been the optical response to a fast rise step in bias field (ref. 18, 10, p. 89, 9, p. 36). The noise suppression scheme of Argyle and Malozemoff (ref. 19) has been incorporated into the system to good effect. In this method the sampling oscilloscope which measures

the output of the photomultiplier is triggered at twice the bias pulse rate. At Monsanto we have accomplished this by triggering on the leading and delayed trailing edge of the pulse by use of an inverting amplifier. A lock-in amplifier, tuned to the basic pulse frequency, then sees an AC signal from the sampling scope of amplitude equal to the difference between the pulsed signal and the background. Thus background ripple, drift, and low frequency noise are effectively eliminated.

This system has sufficiently improved the signal to noise ratio so that it is possible unambiguously to observe oscillations of the domain walls excited by the step drive field. This phenomenon is most pronounced in the low damping Gd-Y garnets but can also be observed as a heavily damped oscillation in some of the Eu-Y-Yb compositions. The application of a modest in-plane magnetic field ($\lesssim$150 Oe) has been found to increase the frequency and assist the observation of this effect. This is accomplished by means of permanent magnets located at predetermined distances from the sample. Even in the absence of oscillations the mobility is significantly enhanced by such a field. Since an in-plane drive field of up to 40 Oe is required in devices we have investigated its effect on mobility and report on it in the appropriate sections.

Temperature Effects

The means of measuring the Neel Temperature using a microscope hot stage and optical detection has been discussed previously (ref. 10, p. 130). Compensation temperatures were measured in somewhat similar fashion where, however, no microscope was used. Instead, light was conducted to the sample by means of a fiber optic "light pipe", then polarized, sent thru the sample, analyzed, and brought out to a photomultiplier via another light pipe. The sample was in a coil within a Dewar vessel where its temperature was adjusted by means of location in the Dewar and a heater coil. The coil provided an alternating bias field and the synchronous optical signal served as a measure of the state of the sample. At compensation the phase of the optical signal changes by 180° generally accompanied by a temperature range in which coercivity is high and therefore small or zero signal is obtained. A substantial drive field was applied to keep the range of small or zero output $\lesssim$10°C and the compensation temperature was taken as the center of this range.

Determination of temperature effects on characteristic length, saturation magnetization, and mobility near room temperature involved the use of a thermoelectric variable temperature stage in the microscope. Such an addition made these measurements possible over a range from -10 to +60°C.

5. THE Gd-Y SYSTEM

Introduction

The mixed Gd-Y magnetic garnets were originally chosen as the subject of this investigation. These garnets are of interest in magnetic bubble technology because the Gd and Y ions have no orbital angular momentum. Therefore, the magnetic garnets are expected to exhibit high domain wall mobilities. In addition, Y-rich compositions can be deposited as epitaxial films on commercially available, high-quality $Gd_3Ga_5O_{12}$ substrates. Also, since the uniaxial anisotropy of the films is primarily stress-induced, a study of the properties of this system permits an evaluation of this mode of anisotropy vis a vis systems exhibiting growth induced anisotropy. Finally, the mixed garnets can be prepared by CVD as well as LPE. Therefore, the system affords a comparison of the relative merits of these methods of preparation.

Film Preparation

Film compositions with gadolinium ions per molecule ranging from 0.2 to 0.6 and gallium ions per molecule ranging from 0.4 to 1.8 were prepared. The films were grown by the isothermal dipping method at temperatures well above 900°C and at relatively low growth rates to minimize lead incorporation. The general growth parameters are given in Table 1. The ratio of $Fe_2O_3 + Ga_2O_3$ to rare earth oxides in solution was 12. Growth temperature was 950-960°C and growth rate was about 0.2 micron per minute.

TABLE 1

GENERAL SOLUTION COMPOSITION

Solvent	92.85 mole %
PbO — 94 mole %	
B_2O_3 — 5 mole %	
Rare Earth Oxides (R_2O_3)	0.65 mole %
Gd_2O_3	
Y_2O_3	
Metal Oxides (M_2O_3)	7.80 mole %
Fe_2O_3	
Ga_2O_3	
$M_2O_3/R_2O_3 = 12$	
Liquidus Temperature ≈980°C	
Growth Temperature 950°C - 960°C	
Growth Rate ≈0.2 μm/min	

In practice, a series of films with constant Gd/Y ratio but with varying gallium content was prepared by adding appropriate increments of Ga_2O_3 to the solution. The films were deposited, without rotation, on Syton-polished (111) GGG wafers of about 1 cm^2 area. Films of different thicknesses were grown for each composition studied; in general, the film thickness ranged from about 3 μm to 7 μm. The thickness variation for a particular film was usually less than ±10% over at least 50% of the total area.

Certain of the films were annealed in air at 1200°C for 15 hours. The granular appearance noted by Cronemeyer et. al. (ref. 20) in annealed films was not observed here - the physical appearance of the films did not change. However, granularity has been observed when other compositions known to contain appreciable amounts of Pb were annealed, indicating a connection of this phenomenon with Pb content of the film. A slight decrease of film lattice constant on annealing was observed.

Results

Anisotropy. - In Figure 4 the uniaxial anisotropy energy density is plotted as a function of strained lattice mismatch for both pre- and post-annealed films grown in tension. Strained lattice mismatch, $\Delta\alpha^{\perp}$, refers to the difference between substrate and film lattice spacings as measured, in situ, in the <111> direction. A non-uniform anisotropy field in the films was found to be related to point-to-point variations in the lattice parameter of the substrates. Differences of as much as 0.0007Å were found in substrates having the characteristic strained core of garnets. Because of the substrate lattice constant variation, the anisotropy was found to vary by as much as 30% from point-to-point in unannealed films on core-free substrates, and by 20% in annealed films. This variation, coupled with the difficulty of measuring the anisotropy, magnetization, and lattice mismatch at the same spot in the films caused significant scatter in the data. The solid lines are drawn to represent the "best" fit to the data. Within the region of sound films, the anisotropy energy increases monotonically with room-temperature lattice mismatch. The films cracked when the strained lattice mismatch exceeded about 0.015Å. The anisotropy in cracked films does not appear to be related to lattice mismatch.

As shown in Figure 4, annealing results in an increase of the anisotropy energy. At least part of this increase can be ascribed to increased strain associated with the slight increase of lattice mismatch caused by the heat-treatment.

It will be noted that the data do not extrapolate to the origin but intersect the abscissa at a lattice mismatch of about 0.007Å. This corresponds to the position of the minimum found by

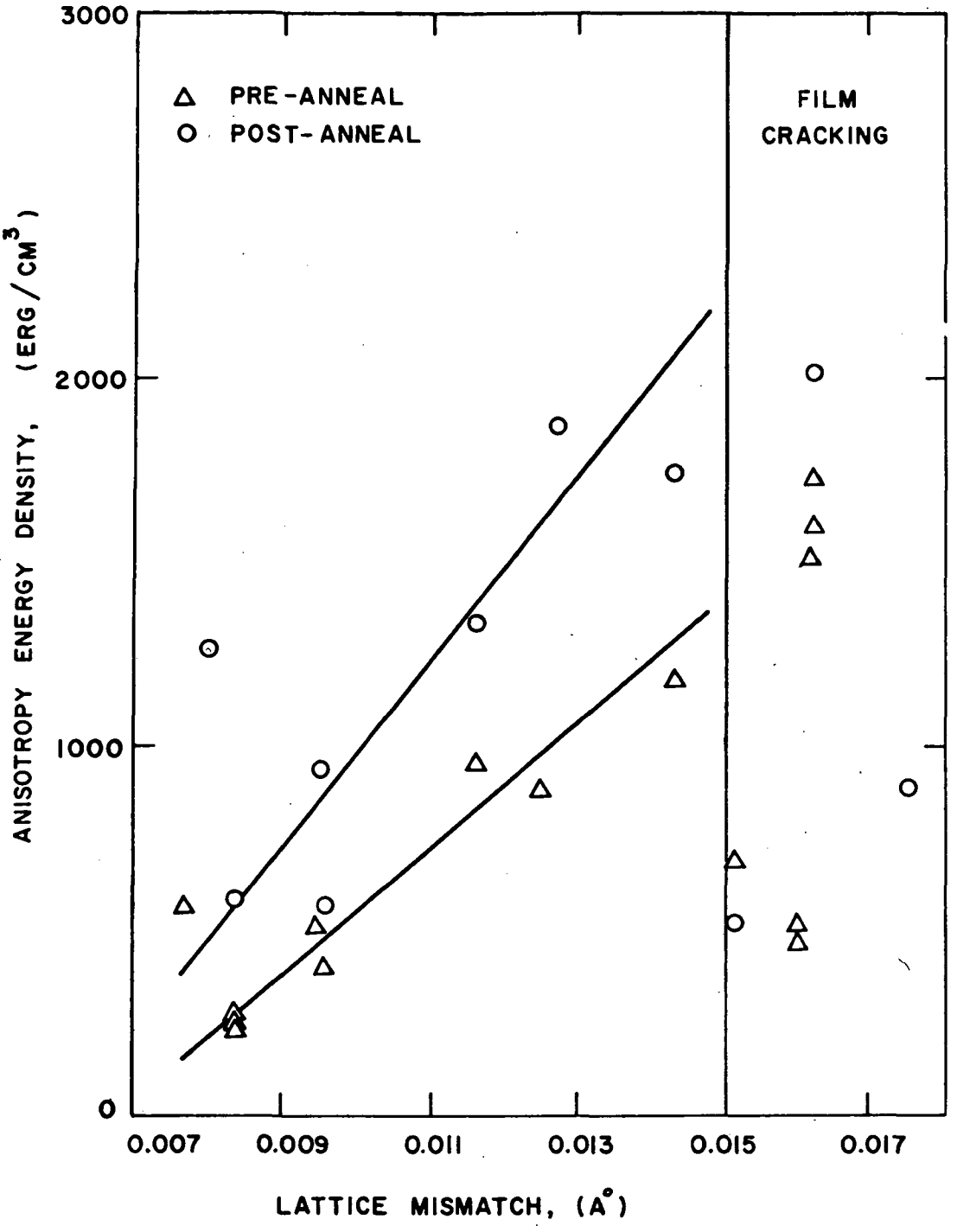

Figure 4. Anisotropy Energy Density vs Strained Lattice Mismatch for Gd-Y Magnetic Garnet Films on GGG Substrates

Stacy, et al. (ref. 21) in anisotropy energy vs misfit strain data for films containing appreciable amounts of Pb. However, the large uniaxial anisotropy observed by Stacy in films in compression was not observed here. This difference in properties is probably due to the difference in the Pb content of the two sets of films. It is believed that the non-zero intercept observed here is due to an in-plane, growth-induced component of anisotropy which was not completely destroyed by the 1200°C anneal. Using values of magnetostriction coefficients and cubic anisotropy derived from extrapolated literature values, the in-plane, growth induced component was estimated to be about 200 Oe in pre-annealed and about 100 Oe in post-annealed films.

In previous work at Monsanto large changes in anisotropy had been effected by annealing Gd-Y films. Such changes were not observed here. It is now believed that the changed observed previously were related to the presence of Pb in the films. The previous films contained 2-3 wt % Pb whereas the concentration of Pb in the present films was less than 0.5 wt %.

Magnetization. - In Figure 5, room temperature saturation magnetization is plotted vs Ga content for films containing various Gd-Y ratios and which exhibited stable domains, In most cases, increasing Ga results in a decrease of magnetization. For the $Gd_{0.6}Y_{2.4}$ compositions, however, stable domains were found only in films with compensation points above room temperature. In these films, magnetization increases with increasing Ga. In addition, comparison of the data of (a) and (b) reveals that the magnetization of the $Gd_{0.6}Y_{2.4}$ films decreased when annealed while the magnetization of films with compensation temperatures below room temperatures increased when annealed.

Transition Temperatures. - The dependence of Neel and compensation temperatures on gallium concentration in both annealed and unannealed gilms is shown in Figure 6. The data shown are for the $Gd_{0.45}Y_{2.55}$ system but are representative of all the compositions studied. The Neel temperature decreased linearly with gallium content and was unaffected by the anneal. The Neel temperatures of the other compositions studied also fall along this line, indicating the Neel temperature is practically independent of Gd-Y ratio over the composition range covered.

The compensation temperature was found to increase with the gallium content of the films and to be especially sensitive to the Gd-Y ratio. Small variations in this ratio are the cause of the scatter in the compensation temperature curves. As is shown in Figure 6, the compensation temperature of all films decreased when the films were annealed and the magnitude of the change increased with increasing Ga. The points on the compensation curves which are marked with crosses represent the extrapolation of the room temperature magnetization vs Ga content curve to zero (Figure 5).

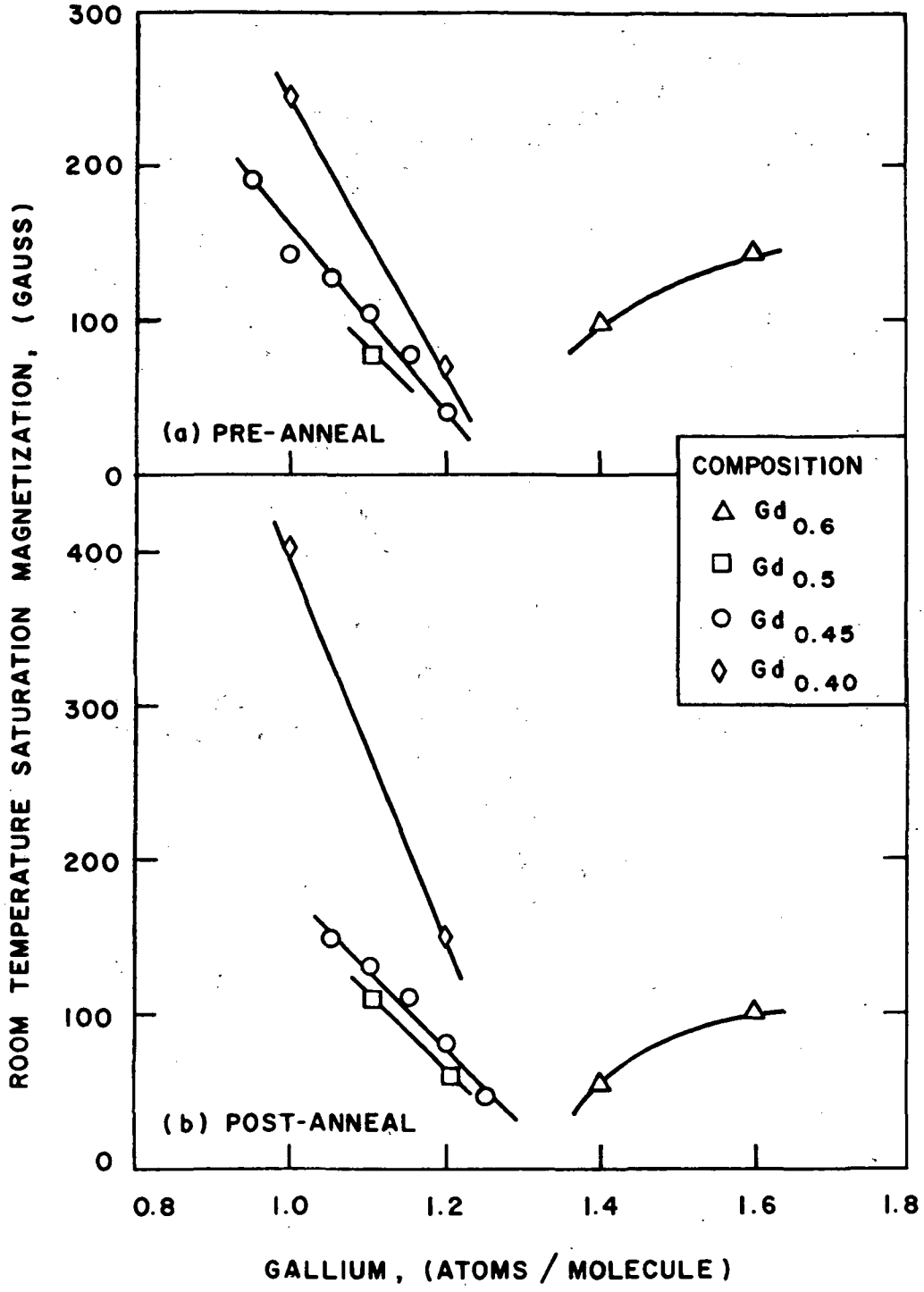

Figure 5. Saturation Magnetization vs Ga Content of Films of Various Gd-Y Ratios

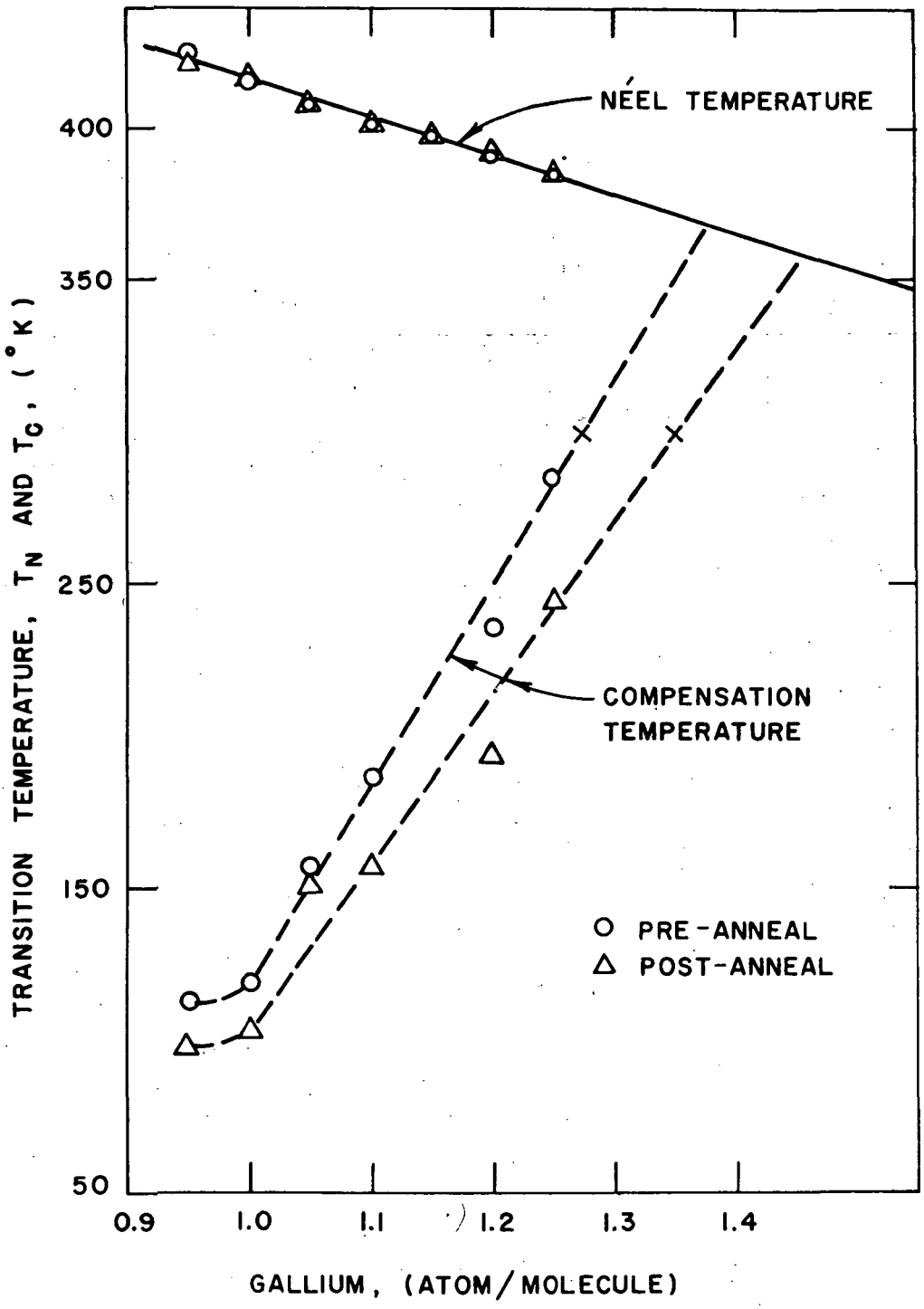

Figure 6. Transition Temperatures vs Ga Content for $Gd_{0.45}Y_{2.55}Fe_{5-x}Ga_xO_{12}$ Films

There is an apparent change of slope in the compensation temperature curves at low temperatures and Ga content. This is probably due to the increasing contribution of the Gd ions to the net magnetization at low temperatures.

Coercivity. - The films were characterized by low values of coercivity which ranged from less than 0.01 to about 0.10 Oe. There was no apparent dependence of coercivity on composition or lattice mismatch.

Temperature Coefficients. - Magnetization of annealed films was measured as a function of temperature from about -5°C to +55°C and the temperature coefficients of the magnetization and characteristic length were calculated for this temperature range. The data are given in Table 2. The most temperature stable compositions are those containing small concentrations of Gd and/or Ga.

Mobility. - The Gd-Y garnets are inherently low damping materials of interest primarily because of their high mobility values (ref. 22,23). Many of these compositions exhibit an underdamped oscillation in an in-plane field such as is shown in Figure 7. Note the very clear increase in oscillation frequency with increasing H_x and the approximate field independence of the decay time of these oscillations. Figure 8 shows these effects more clearly. Here the frequency, f, and decay time, τ_d, of the resonant oscillations measured at 3 spots on the sample of Figure 7 are plotted vs in-plane field, H_x. Frequency is clearly a linear function of H_x except for some tailing off near $H_x = 0$. Such a relationship is well obeyed by all samples studied. Frequency is also quite reproducible from one place to another on the sample. The decay time of the oscillations, on the other hand, shows considerable variation over the specimen and a possible trend toward shorter τ_d at high fields. Since there may be more than 100 strip domains within the field of view at one time, this decay time may merely reflect the loss of phase coherence among that large number of oscillating walls rather than a fundamental damping phenomenon.

The usual treatment (ref. 22) of this phenomenon starts from the harmonic oscillator equation

$$m\ddot{x} + \beta\dot{x} + \alpha x = 2M_S H \qquad (1)$$

and leads to the relations

$$\alpha = 2M_S H_O / x_O \qquad (2)$$

$$m = \alpha / [\omega_r^2 + \tau_d^{-2}] \qquad (3)$$

TABLE 2

PROPERTIES OF ANNEALED $Gd_yY_{3-y}Fe_{5-x}Ga_xO_{12}$ FILMS

Composition		$4\pi M_s$	ℓ	H_A	Temperature Coefficients	
Gd(y)	Ga(x)	(gauss)	(μm)	(Oe)	$\frac{100\Delta M_s}{M_s \Delta T}$	$\frac{100\Delta \ell}{\ell \Delta T}$
0.2*	0.8	396	0.31	200	---	---
0.4	1.0	337	0.31	210	-0.18	-0.17
0.4*	1.2	148	0.72	450	+0.03	-0.91
0.45	1.0	245	0.12	96	+0.03	≈0
0.45	1.05	134	0.38	352	+0.21	-1.35
0.45	1.10	126	0.46	347	+0.16	-1.17
0.45	1.15	113	0.80	451	+0.02	-1.89
0.45	1.20	83	1.15	520	+0.49	-2.53
0.45*	1.25	46	1.41	450	+0.09	-1.79
0.50	1.2	133	1.30	110	---	---
0.50*	1.3	53	1.30	---	+0.59	-3.7
0.60	1.4	47	1.82	240	-2.1	+3.9
0.60*	1.6	99	0.36	172	-2.3	+1.0

* Film Cracked

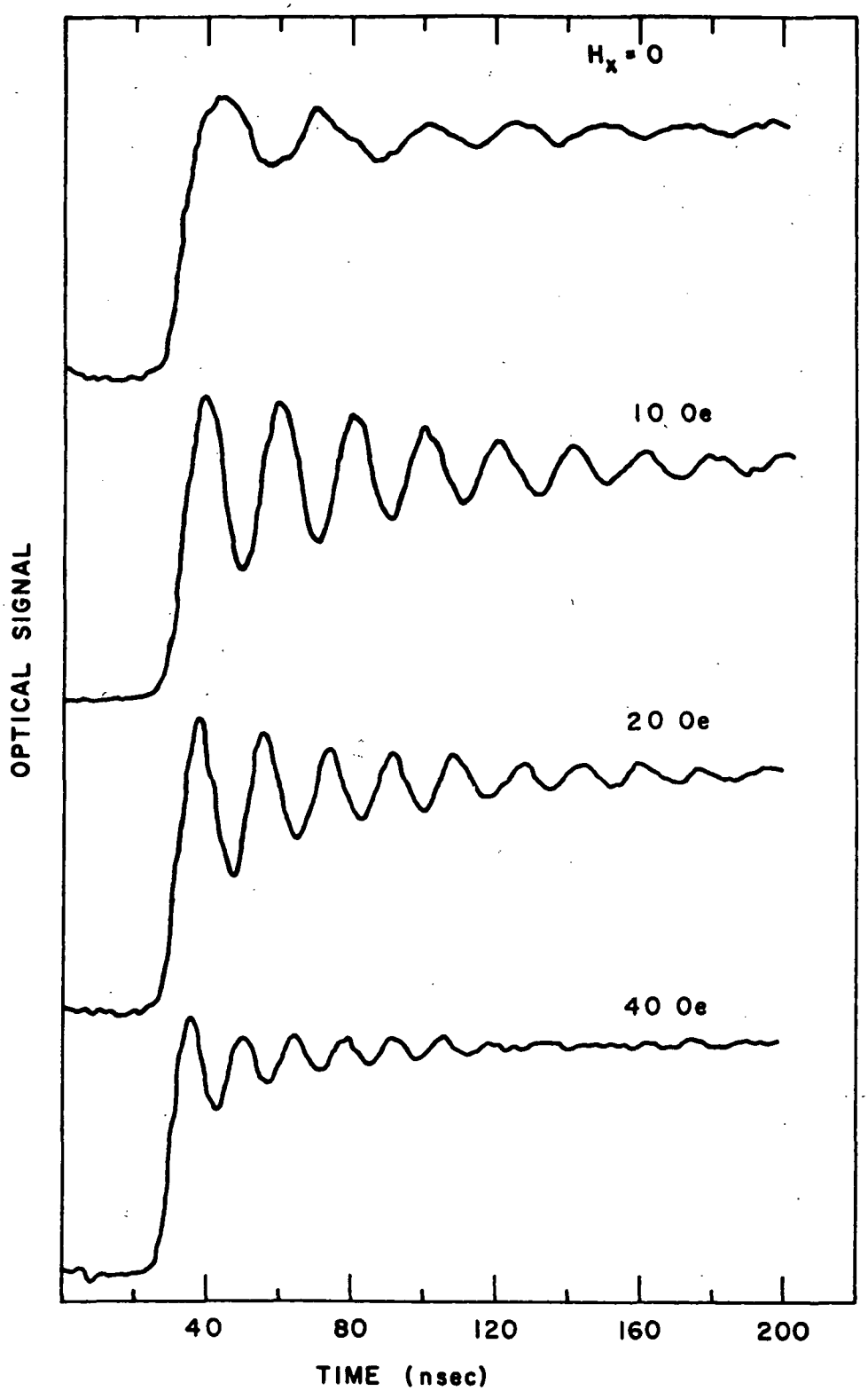

Figure 7. Recorder Tracing Showing Domain Wall Damped Oscillations in the Presence of In-Plane Fields H_x for $Gd_{0.45}Y_{2.55}Fe_{3.9}Ga_{1.1}O_{12}$

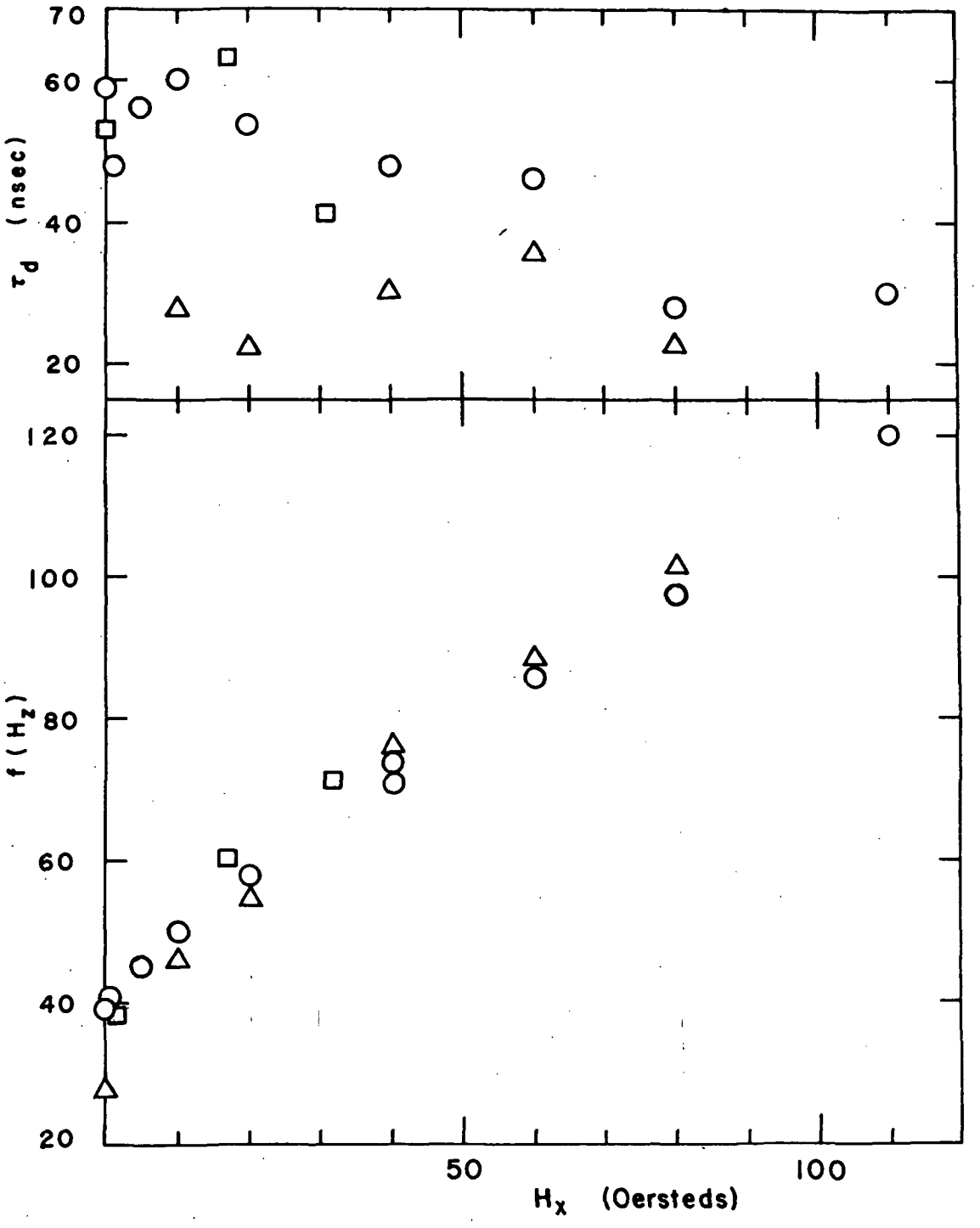

Figure 8. Decay Time and Resonant Frequency vs In-Plane Magnetic Field for Three Locations on $Gd_{0.45}Y_{2.55}Fe_{3.9}O_{12}$ Sample

$$\beta = 2M/\tau_d \tag{4}$$

and $$\mu_w = M_s \tau_d / m \tag{5}$$

Here x_o is a wall displacement corresponding to applied field H_o, ω_r is the angular frequency of the oscillations, τ_d is their decay time, and μ_w is the wall mobility. Based upon this approach the wall mass per unit area for the sample shown in Figures 7 and 8 decreased from 1.04×10^{-10} g/cm^2 at $H_x = 0$ (using the frequency determined from the linear extrapolation of the data to $H_x = 0$) to 0.18×10^{-10} at 80 Oe. Over the same range the mobility increased from approximately 3,000 to 18,000 cm/sec Oe. These values are typical of those obtained on underdamped samples.

Theoretical calculations (ref. 24) yield the equation for wall mass per unit area

$$m_w = \frac{1}{2\pi\gamma^2}\left[\frac{H_A M_s}{2A}\right]^{\frac{1}{2}} = H_A/4\pi M_s \ell \gamma^2 \tag{6}$$

where γ is the gyromagnetic ratio, A is the exchange constant given in terms of earlier parameters by $A = 2\pi^2 \ell^2 M_s{}^3/H_A$ (substituting this yields the last relationship of eq. 6) and the other symbols are as defined above. For the sample discussed above, this yields 5.6×10^{-11} g/cm^2, i.e. the experimental mass is larger than this theoretical value by the factor 1.8. This factor shows considerable variation over the samples studied, ranging from $\sim$1 to 12 with no discernible relationship to other properties.

Discussion

It is well known that the distribution of Ga ions among the tetrahedral and octahedral sites of the garnet lattice is a function of Ga concentration and equilibration temperature (ref. 25). The changes in lattice mismatch, compensation temperature and magnetization of the films reported on here, brought about by the 1200°C anneal, are all consistent with the redistribution of Ga ions among the sublattice sites -- Ga ions being shifted from tetrahedral to octahedral sites by interchange with Fe ions. The result is to decrease the contribution of the tetrahedral sublattice to the net magnetic moment; thus reducing the compensation temperature and causing a change in the saturation magnetization of the films. In addition, there is a shrinkage of the lattice as the small Ga ions are shifted from tetrahedral to the larger octahedral sites.

Some of the properties of the $Gd_yY_{3-y}Fe_{5-x}Ga_xO_{12}$ system are summarized in Figure 9. Here, the Gd(y) concentration is plotted as the abscissa and Ga(x) concentration as the ordinate. The

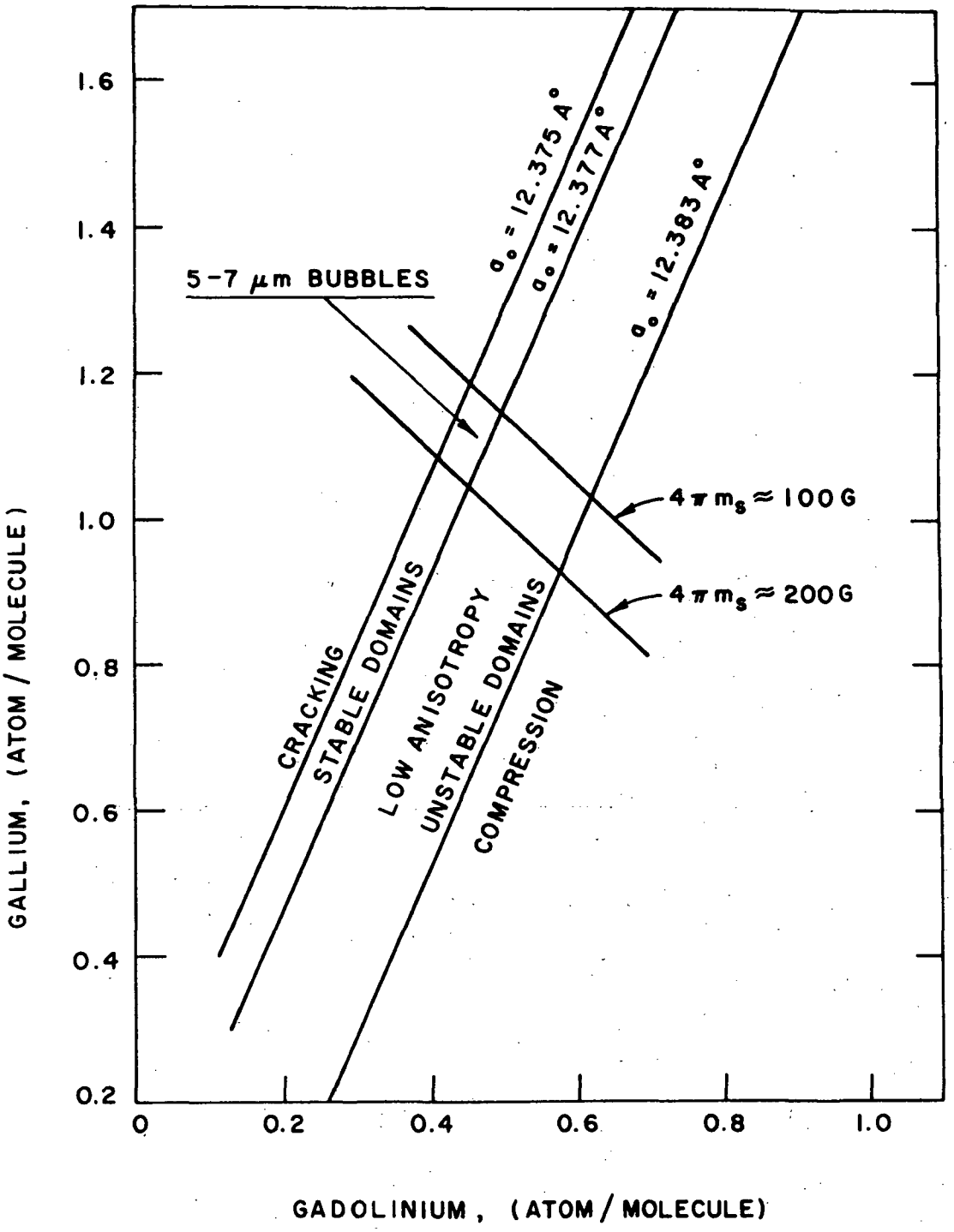

Figure 9. Properties of the $Gd_yY_{3-y}Fe_{5-x}Ga_xO_{12}$ System

lines of constant lattice parameter were calculated by applying Vegard's law to the mixed garnet system. Stable domains were not obtained until the difference was about 0.006Å while film cracking occurred for a difference greater than about 0.008Å. (Note the difference referred to here is the difference between the parameters of the unstrained substrate and film and not the strained lattice mismatch discussed earlier.) Therefore, useful films have a lattice parameter difference range of only about 0.002Å.

Magnetic films which support bubbles of 5-7 μm are of particular interest at the present time. The magnetization of films which support such bubbles range from about 100 to 200 gauss. Film compositions with these properties are indicated in Figure 9.

The films discussed here contain considerably less Pb than LPE films reported on previously (ref. 21,26, and 27). Since Pb expands the garnet lattice, the present films contain higher concentrations of Gd than those films of the same lattice parameter and Ga concentration which contain appreciable amounts of Pb. Furthermore, the anisotropies reported here are, in general, lower than those previously reported. This suggests that Pb introduces an additional component, probably growth-induced, of uniaxial anisotropy normal to the film plane.

Films prepared by CVD do not contain Pb, of course, However, since CVD films are deposited at about 1200°C, it is likely that such films would not exhibit the in-plane growth induced anisotropy postulated here for LPE films.

Although the Gd-Y film compositions exhibit low coercivities and high domain wall mobilities it does not appear that the system is suitable for device application. First, only modest anisotropies were achieved in as-grown films; nor did annealing result in the large increase of anisotropy which was expected. The resultant q factor obtained in 6 μm bubble films (≈4) is considered too low for practical device operation. Domains tend to strip out when circuits are operated on such materials. Second, the temperature coefficient of the characteristic length of 6 μm bubble material is above 1% per degree - a value too high for device use. Lower temperature coefficients could be obtained in compositions containing less Gd and Ga (smaller bubble diameters) but the q values would still be low. Finally, the variation of lattice parameter in even the best available substrates results in a heterogeneous stress-induced anisotropy field in the epitaxial films. Since a fairly complete understanding of the Gd-Y system had been developed, and on the basis of the above considerations, it was decided in consultation with the project monitor to stop work on the Gd-Y system in January 1973 and to devote the remainder of the program to an investigation of a garnet system of more practical interest. The Eu-Yb-Y system was chosen for this study. Its preparation and properties are discussed in Section 6.

6. THE Eu-Yb-Y SYSTEM

Introduction

The following criteria were used in selecting a material to replace the Gd-Y system as the subject of this investigation:

(1) Uniaxial anisotropy in the range 1000 to 2000, preferably growth induced.

(2) Temperature coefficient of characteristic length of less than 0.5% per degree.

(3) Preserve, as far as possible, the high domain wall mobility inherent in the pure $Y_3Fe_5O_{12}$ (YIG) system.

As an addition to the Ga-YIG system, gadolinium was found to have two basic drawbacks: First, as was shown in Section 5, it does not lead to the desired level of uniaxial anisotropy. Second, pure $Gd_3Fe_5O_{12}$ (GdIG) has the highest compensation temperature (T_c) of any of the rare earth iron garnets, approximately 18°C. In keeping with this, the Gd ion has been found to raise T_c of a mixed garnet system quite strongly. Although a compensation temperature is associated with a lower value of the temperature coefficient of $4\pi M_s$, $d\ell/dT$ is unacceptably large for those Gd compositions having desirable bubble size and $4\pi M_s$.

The substitution of a number of ions with lower T_c in their pure iron garnet state had been studied both at Monsanto and elsewhere. In order to simultaneously preserve high mobility, ions with little or no angular momentum are desirable substitutes and Yb, Tm, Lu, La, and Eu satisfy both of these desiderata. Among these $La_3Fe_5O_{12}$ cannot be prepared and of the rest only $Eu_3Fe_5O_{12}$ and $Lu_3Fe_5O_{12}$ exhibit no tendency toward magnetic compensation down to the lowest temperature attainable. Since the lattice constant of Ga-YIG is substantially lower than that of GGG, a large rare earth ion is needed as a substituent which effectively eliminates Lu from consideration. Also mitigating against Lu and La (and in favor of Eu) is the experimentally observed fact that when attempting epitaxy on GGG, rare earth ions having an ionic radius near that of Gd have distribution coefficients more nearly equal to one (see Section 8) than those rare earth ions with ionic radii which differ widely from GGG. In general, it is much easier to obtain reproducibility with a rare earth distribution coefficient near unity. The $Eu_yY_{3-y}Fe_{5-x}$(Ga or Al_xO_{12} system can be conveniently grown on GGG, exhibits growth induced anisotropy of satisfactory magnitude, and has desirable temperature characteristics (ref. 28). The mobility is not as high as that found for GdY garnets (i.e. 200 to 500 cm/sec Oe, rather than ∿2000) but small

additions of Yb have been found to reduce the dynamic instabilities which give rise to velocity saturation at device magnitude drive firlds and the concomitant low mobility values (ref. 28). While it is likely that the EuY garnets with other small additions may not be the final, commercial bubble material, it appears at this time to be an excellent choice for study. Preliminary work previously carried out at Monsanto on EuY garnets indicated that the low Eu end of the system with Ga as a substituent for Fe would be an excellent starting point. Work on this system was initiated in January 1973.

Film Preparation

Film compositions with Eu ions/molecule ranging from 0.4 to 0.6, Yb ions/molecule ranging from 0.05 to 0.4 and Ga ions/molecule ranging from about 1 to 1.5 were prepared. The films were deposited from $PbO-B_2O_3$ solution by the isothermal dipping method. The substrates were mounted horizontally and were rotated during growth. To insure film thickness uniformity rotation rates of 100-200 rpm were used. Thickness uniformity of less than ±1% over most of the film area was usually obtained.

Substrates were Syton-polished (111) GGG wafers. Both "core-free" substrates and those having the characteristic strained core were used. The diameter of the wafer ranged from about 15 to 25 mm.

In practice a series of films with constant rare-earth ratio but with varying Ga content was prepared by adding appropriate increments of Ga_2O_3 to the melt. Growth temperatures ranged from about 950 to about 990°C.

Results

Saturation Magnetization. - In Figure 10 room temperature saturation magnetization is plotted as a function of gallium content for films containing various concentration ratios of the rare-earth ions. Since the films are not of the same or optimum thickness, there is some scatter in the data. However, the general behavior appears obvious. Magnetization decreases with increasing gallium content and does not depend strongly, if at all, on the concentration ratio of rare-earth ions. The decreasing slope (as gallium increases) of the curve in Figure 10 is probably due to the changing distribution of gallium ions among the tetrahedral and octahedral sites of the garnet lattice as total gallium content increases.

Characteristic Length. - The behavior of characteristic length, ℓ, with composition is illustrated in Figure 11. Since ℓ is a

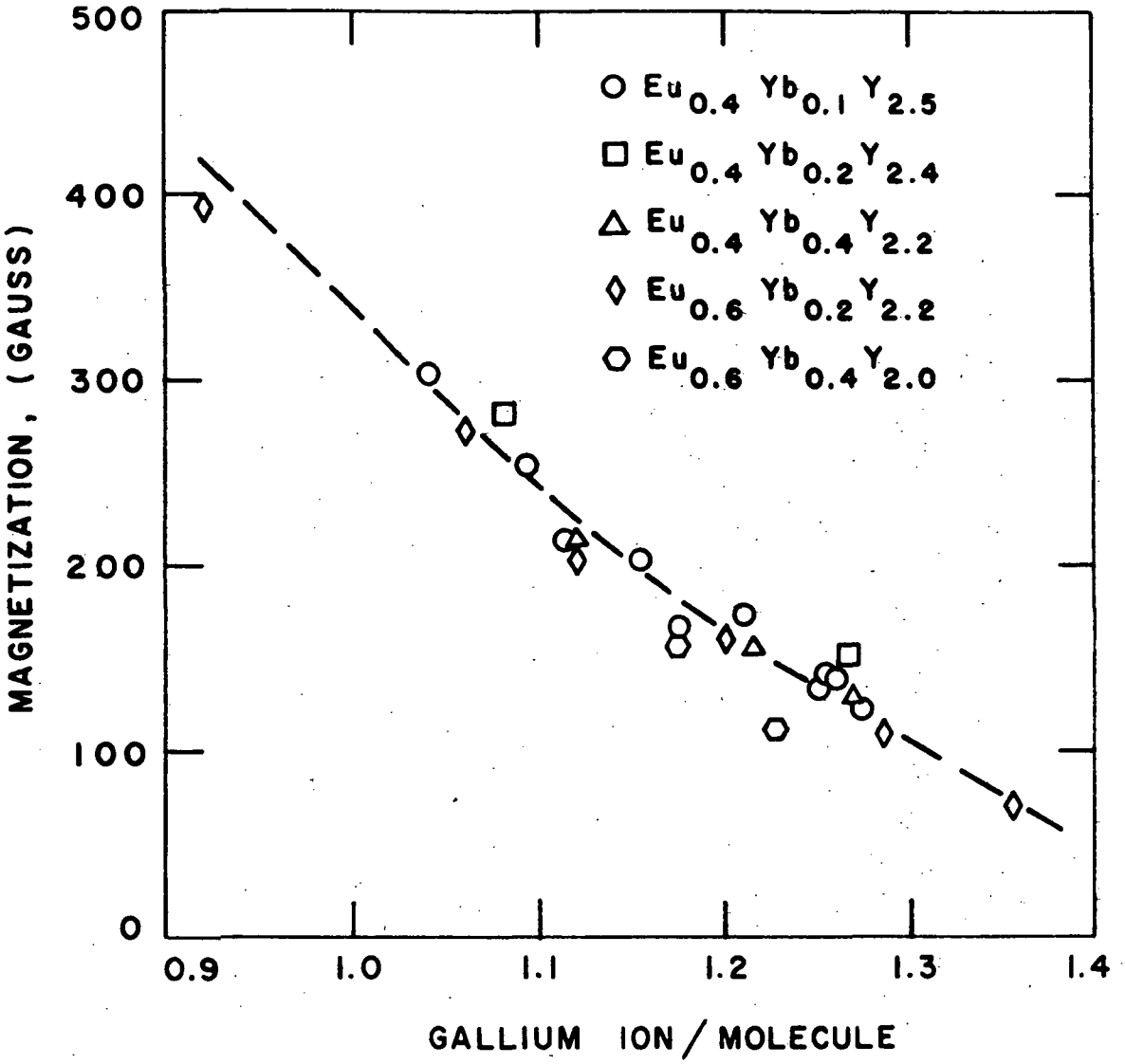

Figure 10. Saturation Magnetization vs Ga Content of Films of Various Eu-Yb-Y Ratios

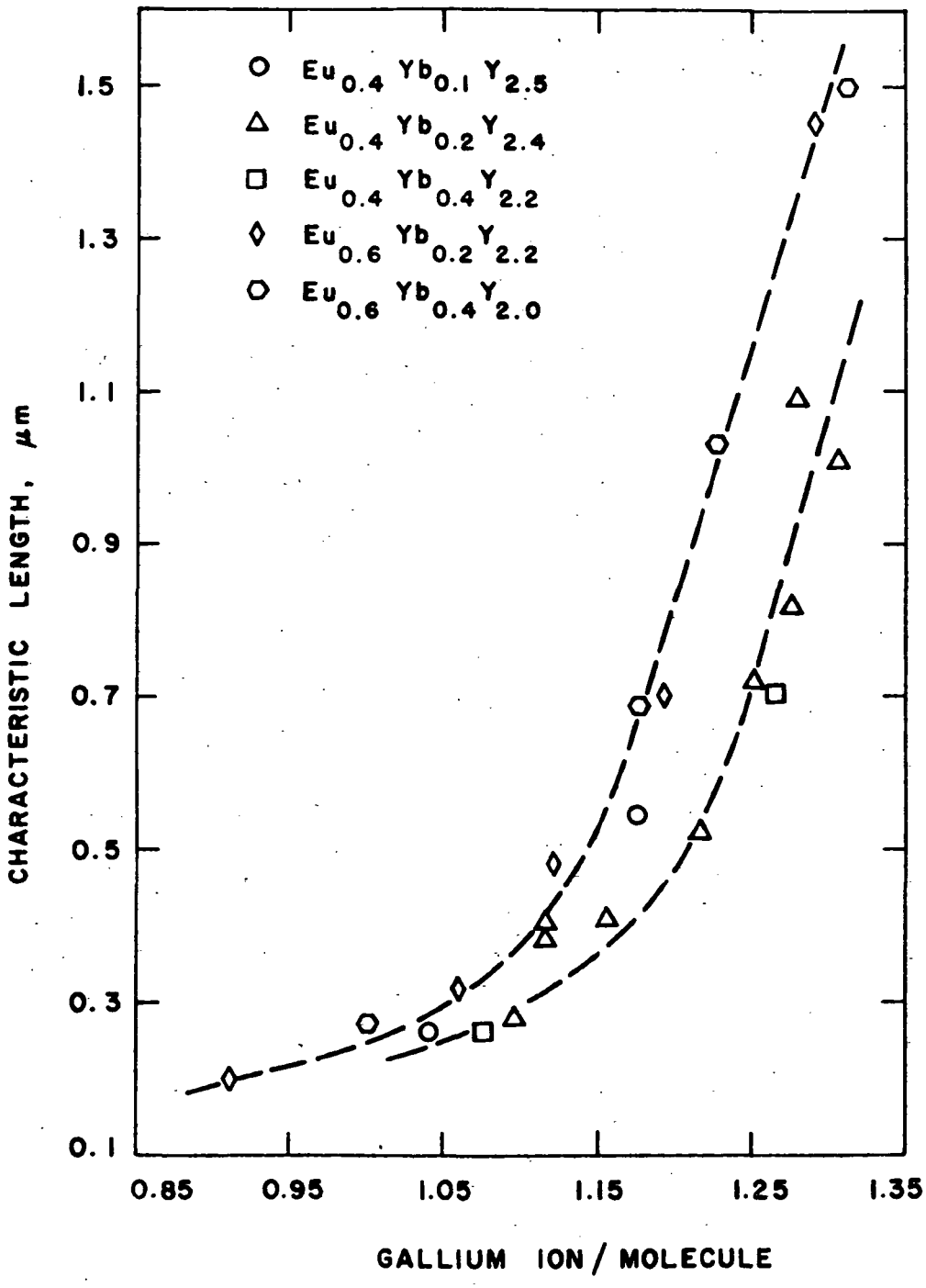

Figure 11. Characteristic Length vs Gallium Content of Films of Various Eu-Yb-Y Ratios

sensitive function of film thickness, there is considerably more scatter here than in Figure 10. However, the data group naturally along two different curves which are related to the Eu content of the films. A higher Eu concentration leads to a larger ℓ. This behavior is consistent with the higher anisotropies associated with higher Eu concentrations pointed out in the following section.

Anisotropy. - The anisotropy field, H_A, and the anisotropy energy density for a number of compositions are given in Table 3. These films were grown at somewhat different temperatures and growth rates and since anisotropy is dependent on these growth conditions, the data are not strictly comparable. However, the values are illustrative of the magnitude of the anisotropy which can be obtained with these compositions. In addition, two composition/anisotropy trends seem to be indicated. First, for a particular rare earth ratio, the anisotropy energy falls with increasing Ga even though the anisotropy field increases. This is a consequence of the rapid decrease of magnetization with Ga content (Figure 10). Second, in general, higher anisotropy appears to be related to higher Eu concentration.

The anisotropy field of films which support 6 μm bubbles range from about 800-2000 Oe-values which are reasonable for device applications. Since the precise value depends on composition and growth conditions, this garnet system affords an opportunity of "tailoring" the anisotropy to a particular value.

Coercivity. - In other work at Monsanto it has been observed that Eu-containing films often exhibit relatively high coercivities. This is in general true of the particular system studied here. However low coercivities can be obtained. Figure 12 is a plot of the coercivities of a number of films vs Ga content. The coercivity increases slowly with increasing Ga to about $x = 1.3$, after which it rises sharply. This behavior is believed to reflect the lattice mismatch between film and substrate. The films are grown in tension and lattice mismatch increases with increasing Ga. It is likely that the lattice constant of films with low coercivity (<0.10 Oe) is a close match to the lattice constant of the substrate. If this is true, then, for a particular Ga content (or bubble diameter) the rare-earth ratio of the composition could be adjusted to provide a close lattice match and, hence, yield a low coercivity.

Temperature Coefficients. - The temperature coefficient of the characteristic length ($100\ \Delta\ell/\ell\Delta T$) was investigated as a function of composition. Results are shown in Figure 13. Here the average temperature coefficient between 0 and 50°C is plotted vs Ga content for various rare-earth ratios. The coefficient is relatively independent of rare-earth ratios but increases rapidly with increasing Ga. The temperature coefficient of films which support stable 6 μm bubbles ($x = 1.2$) is about 0.5% per degree.

TABLE 3

UNIAXIAL ANISOTROPY OF SOME Eu-Yb-Y FILMS

Sample Number	Composition				Magnetization (Gauss)	Anisotropy Field (Oe)	Anisotropy Energy (erg/cm^3)
	Eu	Yb	Y	Ga			
34534A	0.4	0.1	2.5	0.97	368	800	10600
34535A				1.04	303	725	9300
34538A	0.4	0.2	2.4	1.07	282	725	9000
34539B				1.11	229	775	7100
				1.28	115	1315	6000
34541C	0.4	0.4	2.2	1.00	331	1050	13800
34542A				1.12	215	1250	10700
34544A				1.27	124	2075	10300
34547A	0.6	0.2	2.2	1.06	273	1070	11600
34548A				1.12	206	1440	11700
34549A				1.20	163	1740	11200
34550A				1.28	110	2520	11000
34555A	0.6	0.4	2.0	1.00	328	1050	13600
34557A				1.22	161	2310	14800
34558A				1.31	91	3150	11400

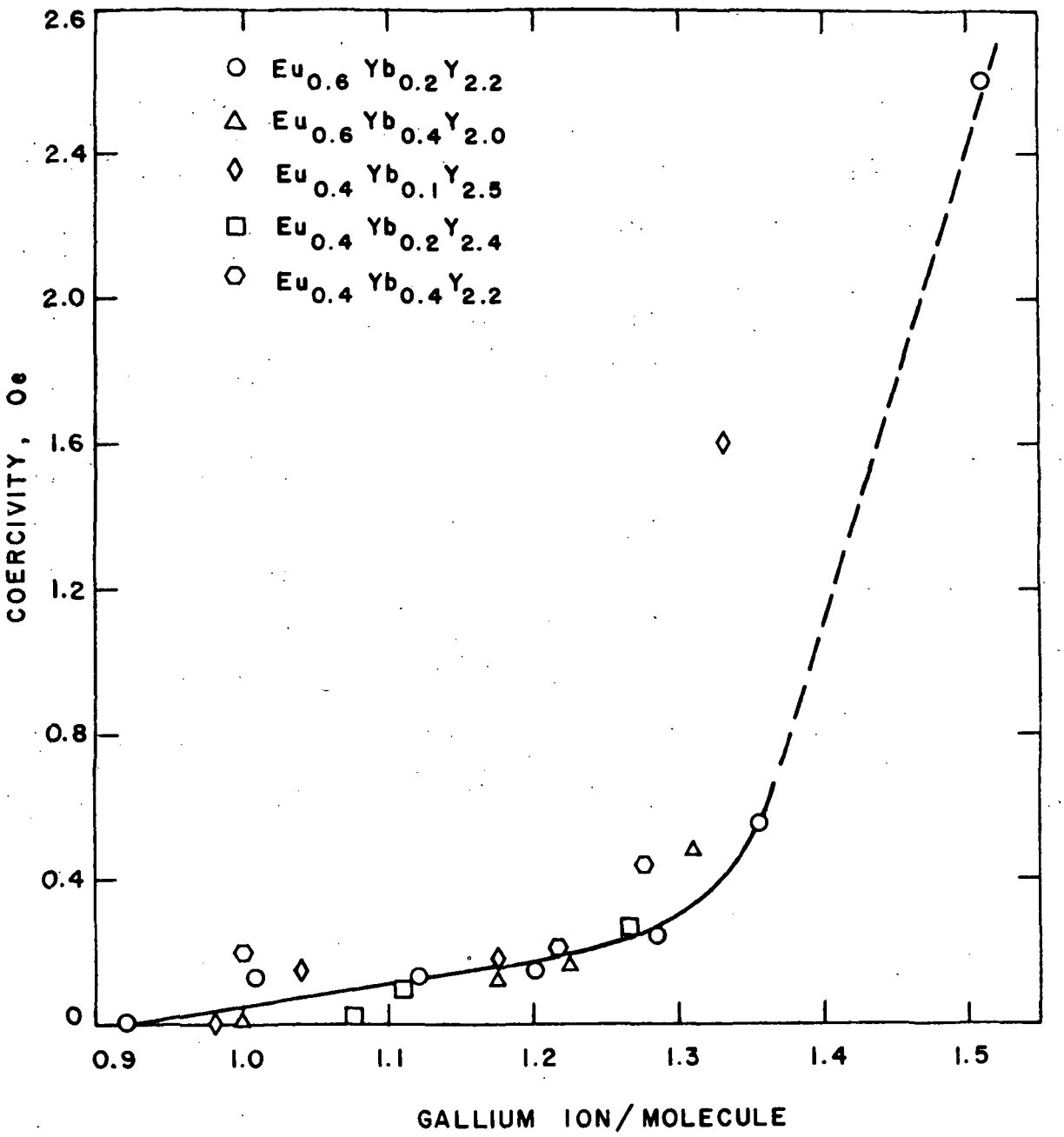

Figure 12. Coercivity vs Ga Content of Films of Various Eu-Yb-Y Ratios

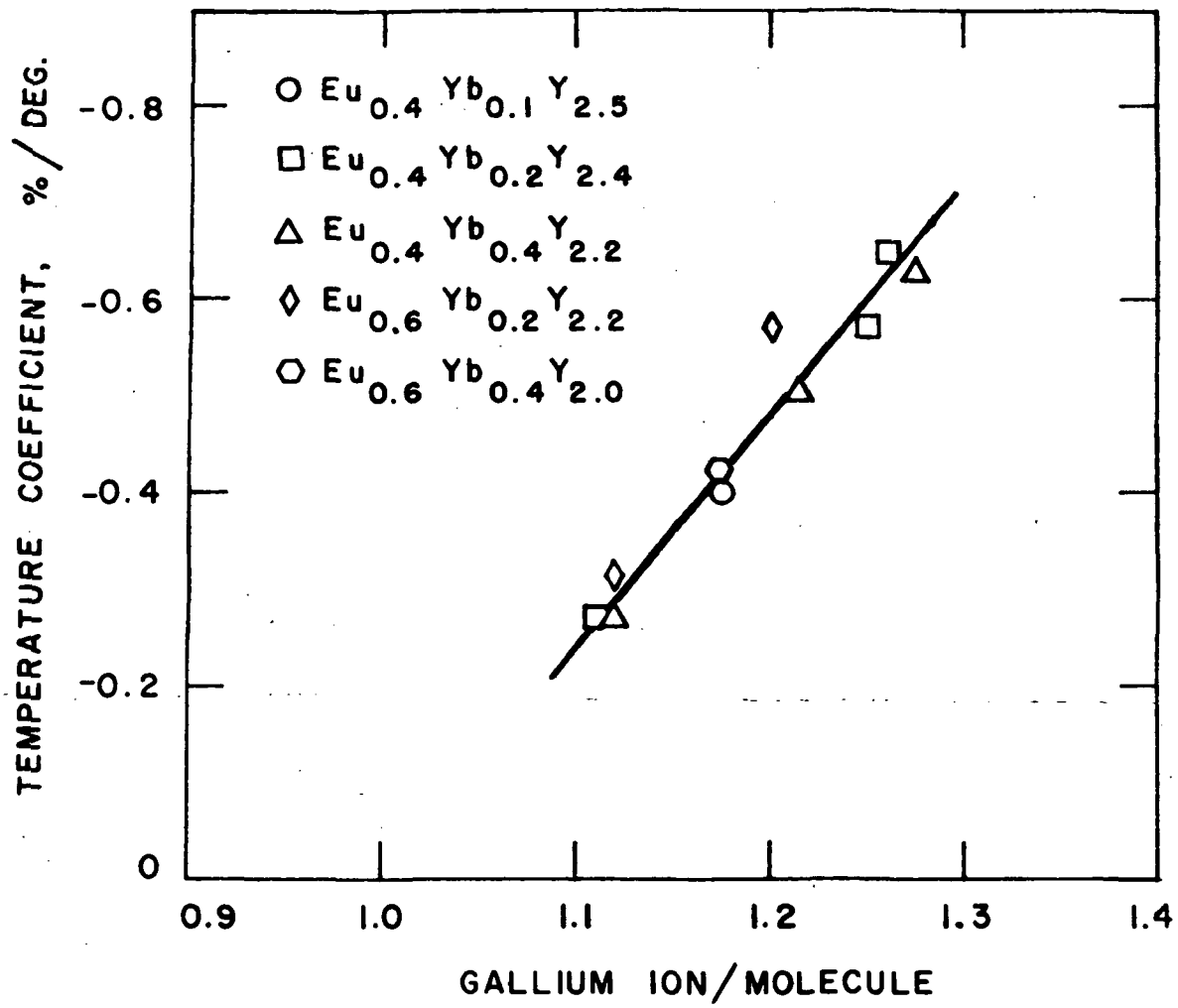

Figure 13. Temperature Coefficient of Characteristic Length vs Ga Content of Films of Various Eu-Yb-Y Ratios

Mobility. Mobility appears to be quite variable, both within one sample and from sample to sample of a given growth series. This effect has been previously reported by Vella Coliero (ref. 29) and has been thoroughly verified in the present study. While no definitive co-relation with other properties has been found, certain trends are detectable.

The response of EuY garnets containing small amounts of Yb to a step change in bias field is exemplified in Figure 14. The response at zero in-plane field is, in this case, clearly charcteristic of an overdamped harmonic oscillator and is treated as discussed in ref. 10, p. 89. Upon application of an in-plane field of 40 Oe or more, heavily damped oscillations are observed which permit analysis of the type discussed in Section 5. The frequency and decay time of these oscillations show behavior similar to that of the GdY garnets, although they are known with less precision. This is illustrated for another sample in Figure 15. Once again there is a reasonably linear frequency vs H_x characteristic which is consistently observed. The internal agreement of the τ_d data must be considered largely fortuitous.

Figure 16 illustrates the behavior of the mobility with in-plane field as determined both from the oscillatory behavior and the over-damped results, where these have been observed. The oscillatory result at $H_x = 0$ is determined from the extrapolations shown in Figure 15. We tentatively assign the difference between these results to a suppression of turbulent motion of the wall by the in-plane field (ref. 19). The presence of an in-plane drive field in a device will clearly improve the speed of the device. If the maximum improvement is desired, however, a better understanding of this phenomenon and great care in film growth will be necessary.

The dependence of mobility on Yb content is considerably confused by the wide variability within one composition. The following general conclusions can be made, however.

(1) For $H_x = 0$ a peak $\mu_w \sim 600$ cm/sec-Oe is attained near Yb = 0.2 atoms/formula unit.

(2) At $H_x = 40$ Oe the lower Yb compositions experience more mobility enhancement leading to a peak μ_w ~ 1500 cm/sec Oe at Yb ~ 0.1 atoms/formula unit.

If lower drive fields were anticipated, an intermediate Yb content would be advisable.

The zero field domain wall mass, which can also be determined from the extrapolations of Figure 15, again exceeds the value given by eq. 6. In the present Eu-Y-Yb garnets the ratio ranges

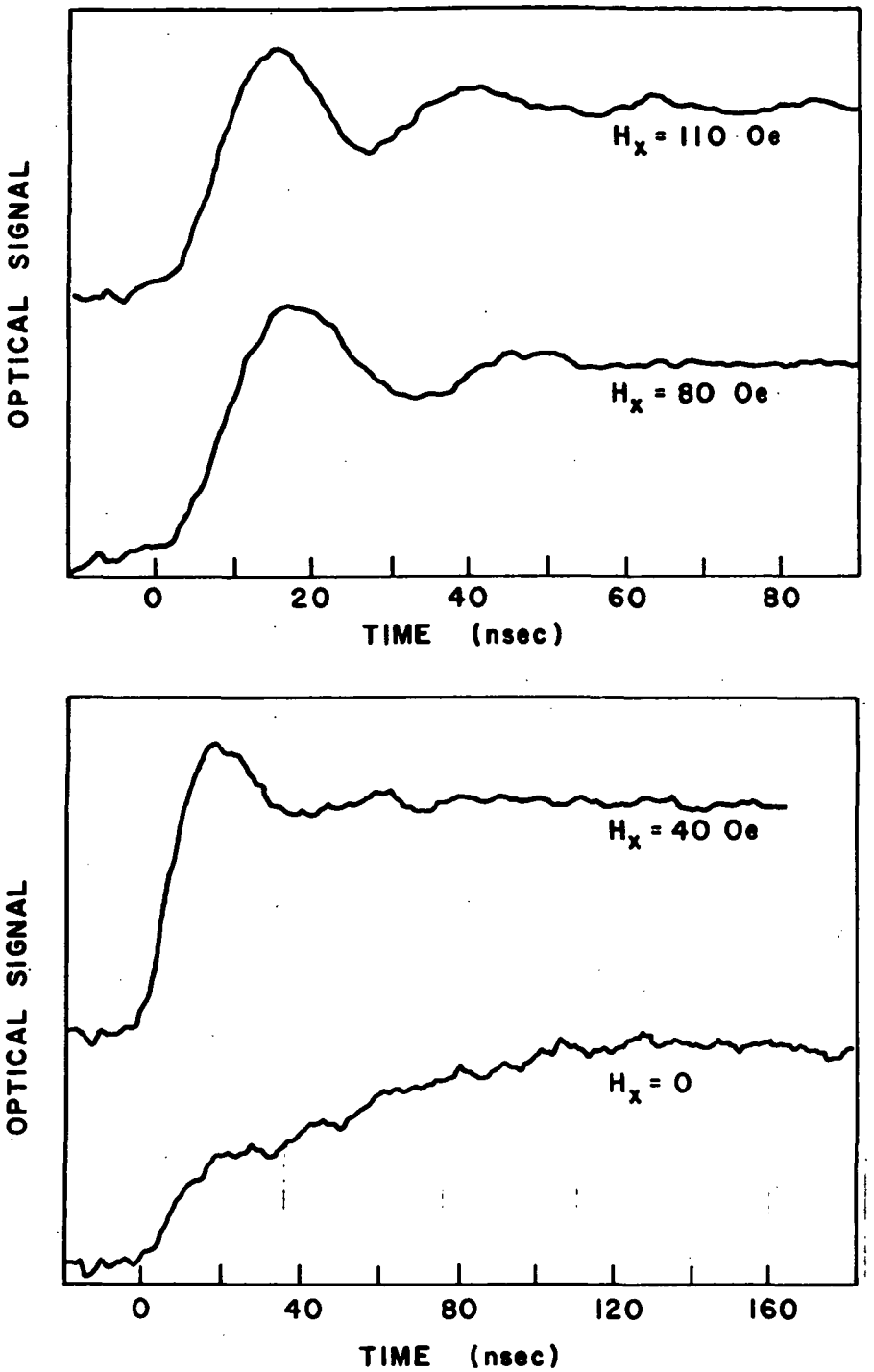

Figure 14. Optical Response of a Sample of $Eu_{0.4}Yb_{0.1}Y_{2.5}Fe_{3.78}Ga_{1.22}O_{12}$ to a Step Rise in Bias Field at Various In-Plane Fields

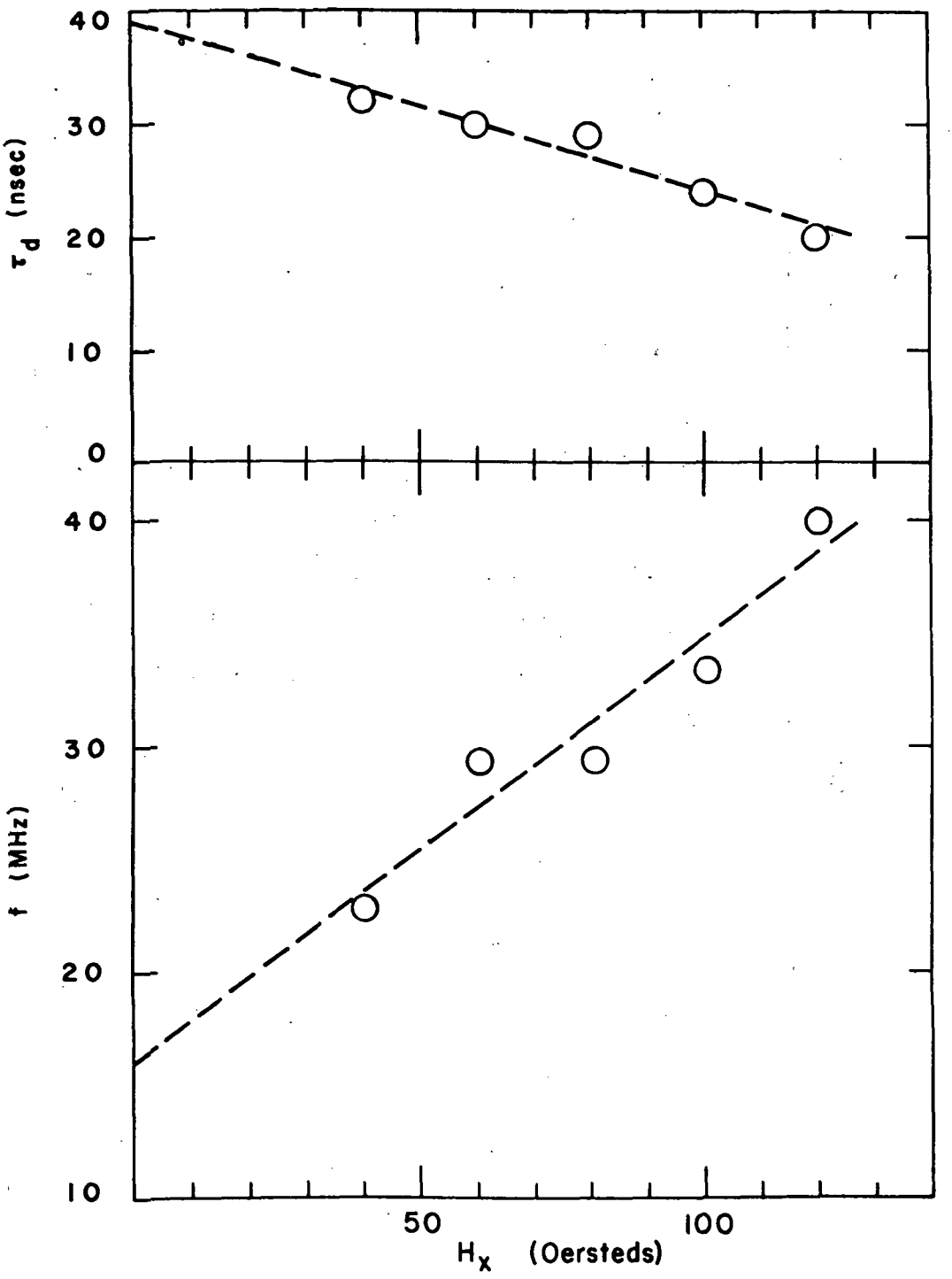

Figure 15. Natural Frequency and Decay Time vs In-Plane Field for a Sample of $Eu_{0.4}Yb_{0.1}Y_{2.5}Fe_{3.78}Ga_{1.22}O_{12}$

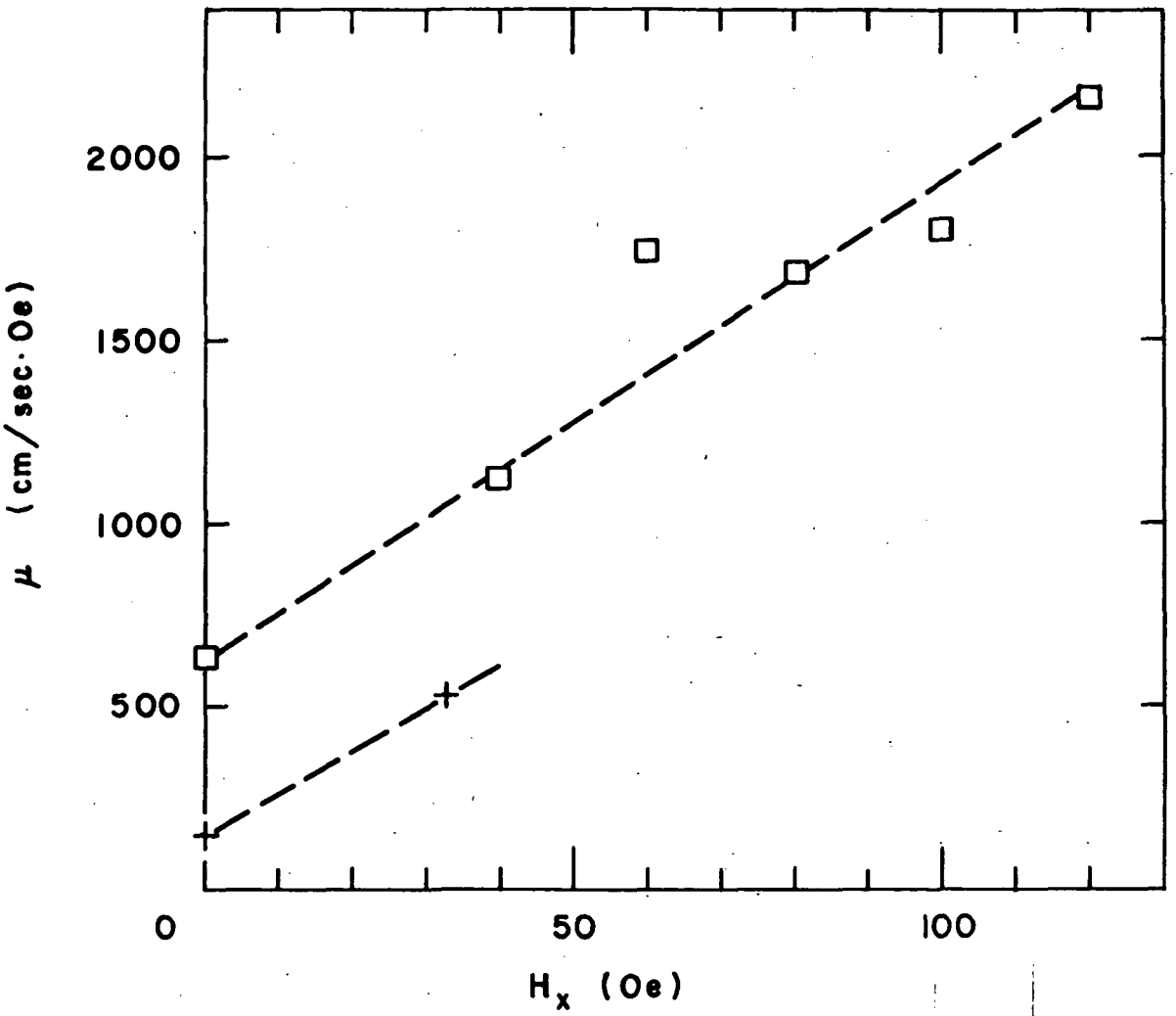

Squares - Results from Oscillatory Response Curves and (at $H_x = 0$) an Extrapolation of Those Results
Crosses - Results from Overdamped Response Curves

Figure 16. Domain Wall Mobility vs In-Plane Field for a Sample of $Eu_{0.4}Yb_{0.1}Y_{2.5}Fe_{3.78}Ga_{1.22}O_{12}$

from about 2 to 8 with little, if any, correlation to other macroscopic parameters. While the existence of ratios significantly greater than one may have a ready explanation in the wall distortions discussed by Schloemann (ref. 30), the variability of this ratio remains a mystery at present.

Temperature Variation of Mobility. - The variation of mobility with temperature has not been a standard measurement in this study because of the various equipment complexities involved. It is, nonetheless, an important characteristic of any material destined for use over a significant temperature range. We have therefore recently initiated such measurements using the step field response method within a thermoelectric variable temperature stage.

Mobility was found to decrease as temperature was lowered, as is shown in Figure 17. For the compositions most thoroughly studied (Yb content of 0.05 and 0.1 atoms/formula unit in Eu-Y-Yb) the wall mobility in H_x = 0 at -10°C ranges from 50 to 150 cm/sec Oe. Application of an in-plane field continues to markedly improve this property. For H_x = 33 Oe (limited by the variable temperature apparatus) low temperature mobilities between 180 and 500 cm/sec Oe were observed, there being a definite correlation between values for H_x = 0 and those for H_x = 33 Oe. There are, in addition, some interesting correlations between low coercivity and high mobility values within this system which should be further studied. Possibly both of these desirable properties are associated with the absence of a very small scale network of defects. Such a network, when present, might not only hold up domain walls , thereby increasing coercivity, but also cause the wall motion to be more turbulent and thus reduce mobility. This network might arise at the film-substrate interface from a lattice mismatch of substrate and film too small to produce cracking. Time has not permitted a full investigation of this point.

Discussion

The Eu-Yb-Y system appears to be a promising candidate for bubble device application. These garnets exhibit reasonable mobilities, satisfactory quality factors and good temperature stability. The composition can be tailored easily to provide a film with certain desired properties. For example, consider optimizing the properties of a film supporting stable 6 μm bubbles in a 6 μm thick film. Assume that a Ga content of 1.2 ion/molecule were required to produce bubbles of the desired size. Maximum mobility is obtained with an Yb content of about 0.15 ion/molecule. Coercivity can be minimized by assuring a close lattice match between film and substrate. This can be accomplished by adjusting the Eu/Y ratio. If the substrate had a lattice constant of 12.383, the desired film composition: $Eu_{0.63}Yb_{0.15}Y_{2.22}Fe_{3.8}Ga_{1.2}O_{12}$ is

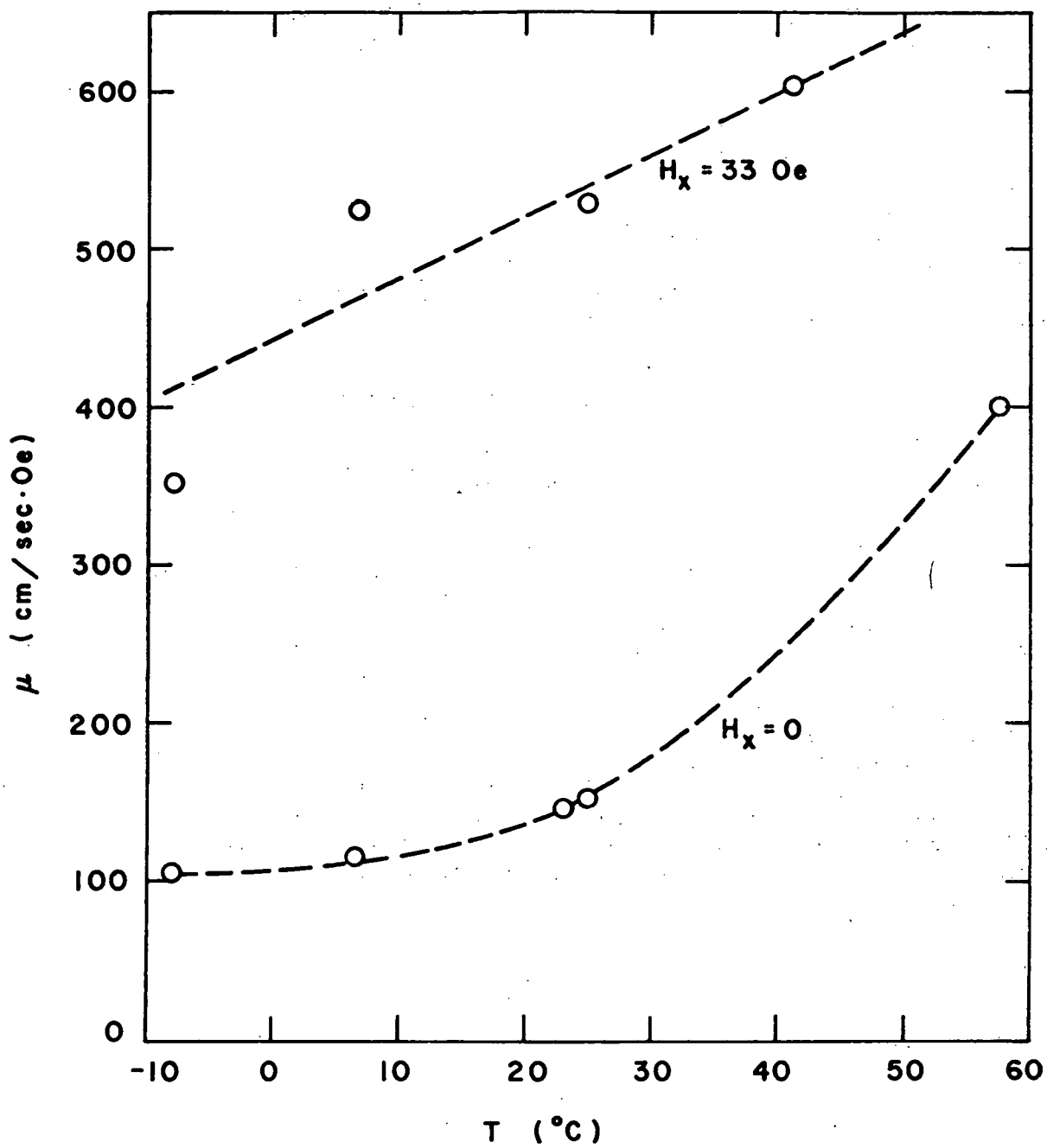

NOTE: All Results are Overdamped Response Curves

Figure 17. Domain Wall Mobility in a Sample of $Eu_{0.4}Yb_{0.1}Y_{2.5}Fe_{3.78}Ga_{1.22}O_{12}$ vs Temperature

arrived at by employing Vegard's law. The temperature coefficient of the characteristic length would be about 0.5% per degree for this composition.

Although a good understanding of this system has been obtained, additional work is needed. The relation between mobility and composition is not entirely clear. In addition, the proposed relation between mobility and coercivity deserves further study. Such a relationship would have an important bearing on bubble technology regardless of film composition. A detailed study might lead to a clearer understanding of wall mobility and wall turbulence in garnet films.

7. GGG SPACING LAYER

Introduction

In a bubble device, the permalloy circuit is separated from the magnetic film by a thin, non-magnetic spacing layer. Usually, SiO or SiO_2 is employed for this purpose. However, the thermal expansion coefficients of these materials do not match the expansion coefficient of the garnet, and, hence, the materials may not be suitable for use as spacing layers in devices subjected to wide temperature excursions. It was an object of this program to investigate a substrate-magnetic film-spacing layer system that was, potentially, more compatible. Specifically, it was proposed to determine the feasibility of depositing, by LPE, $Gd_3Ga_5O_{12}$ spacing layers on the magnetic films. It was reasoned that a magnetic film sandwiched between a substrate and spacing layer of the same composition would provide a closer approach to the ideal composite structure.

Experimental

Since the Ga garnets are more congruently saturating in PbO-based solvents than are the Fe garnets, the large R_1 (metal oxide/rare-earth oxide ratio in solution) which is necessary to deposit Fe garnets is not required for the Ga garnets. In fact, R_1 ranging from 1.67 (stoichiometric) to 12 were used in this work with equally satisfactory results. An R_1 of 5.5 and a Gd_2O_3 concentration of about 0.7 mole percent was used for most of this work. The films were grown by the isothermal dipping method at about 915°C. Films were grown both statically and with rotation. The best thickness uniformity was achieved by growth with rotation. Films were deposited on Syton-polished GGG substrates as well as on a variety of magnetic film compositions.

Results

The lattice constant of LPE-grown films of GGG is significantly smaller than that of Czochralski-grown GGG. The lattice constant of the films measured in situ on Czochralski grown GGG substrates is 12.378Å while that of the substrate is 12.383Å. The lattice constant of the film is close that (12.375Å) reported for polycrystalline GGG prepared by solid state reaction of appropriate oxides (ref. 31). The difference in the lattice constant of the GGG film and substrate is probably due to stoichiometric differences as discussed by Geller, et. al. (ref. 32). Czochralski-grown GGG apparently contains a small excess of Gd ions on Ga sites which results in the larger lattice constant.

As expected, the physical perfection of the spacing layer was related to the perfection of the underlying magnetic film. Dislocations, scratches, etch pits or other physical imperfections present in the magnetic film are propagated into the spacing layer just as imperfections in the substrate are propagated into the magnetic film.

The severity of defecting appeared to depend on the relative lattice constants of substrate, magnetic film and spacing layer. Defect formation was exaggerated if the lattice constants of the respective components differed too greatly. This is illustrated by the data of Table 4 which lists the lattice constants (a_o) and thicknesses (h) of the components of several composite structures. (The lattice constant of all spacing layers in Table 4 is assumed to be 12.378Å.) Best results were obtained when the spacing layer was deposited on a magnetic film having nearly the same or slightly larger lattice constant (Samples 34530I, 34533C, and 34533D).

The presence of the GGG spacing layer did not appear to affect, significantly, the magnetic properties of the bubble domain film.

Permalloy propagation circuits were fabricated on $Gd_{0.9}Er_{2.1}Fe_{4.4}Ga_{0.6}O_{12}$ magnetic film -- GGG spacing layer combinations and domains were propagated readily. The GGG spacing layers appear to be superior to SiO and SiO_2 in at least three respects: (1) circuit fabrication time is reduced, (2) GGG absorbs less in the visible spectrum resulting in better visibility, and (3) spacing layer adherence is superior and is as good as substrate-magnetic film adherence.

Discussion

This work has demonstrated that it is feasible to deposit GGG spacing layers by LPE on magnetic garnet films. With proper lattice constant matching, the GGG substrate-magnetic film-GGG spacing layer composite is superior in important respects to the structures in

TABLE 4

PROPERTIES OF GGG SUBSTRATE - MAGNETIC FILM - GGG SPACING LAYER COMBINATIONS

Sample Number	Substrate a_o	Magnetic Film Composition	h	a_o	Spacing Layer h	Remarks
34530C	12.3838	$Eu_{0.4}Y_{2.6}Fe_{4.8}Ga_{1.2}O_{12}$	4.99	12.372	4.4	Many Defects
34530D	12.3830	$Eu_{0.4}Y_{2.6}Fe_{4.8}Ga_{1.2}O_{12}$	4.40	12.372	7.0	Many Defects
34530E	12.3830	$Eu_{0.4}Y_{2.6}Fe_{4.8}Ga_{1.2}O_{12}$	5.73	12.372	2.6	Moderate Defects
34530F	12.3844	$Eu_{0.4}Y_{2.6}Fe_{4.8}Ga_{1.2}O_{12}$	4.60	12.372	1.05	Some Defects
34530G	12.3838	$Eu_{0.4}Y_{2.6}Fe_{4.8}Ga_{1.2}O_{12}$	6.18	12.372	---	Faceted Layer
34530H	12.3838	$Gd_{1.1}Y_{0.9}Tm_{1.0}Fe_{4.35}Ga_{0.65}O_{12}$	5.51	≈12.387	0.730	Many Defects
34530I	12.3838	$Gd_{0.45}Y_{2.55}Fe_{3.9}Ga_{1.1}O_{12}$	5.33	≈12.376	0.983	Few Defects
34533C	12.3844	$Eu_{0.6}Y_{2.4}Fe_{3.7}Ga_{1.3}O_{12}$	1.34	≈12.382	3.13	Few Defects
34533D	12.3844	$Eu_{0.6}Y_{2.4}Fe_{3.7}Ga_{1.3}O_{12}$	3.38	≈12.382	2.82	Few Defects
34560C	12.3838	$Gd_{0.9}Er_{2.1}Fe_{4.4}Ga_{0.6}O_{12}$		≈12.378	5.84	Few Defects
34560E	12.3838	$Gd_{0.9}Er_{2.1}Fe_{4.4}Ga_{0.6}O_{12}$		≈12.378	1.36	

common use today. The GGG spacing layer could not be employed, of course, if ion implantation is used to "hard-bubble proof" the magnetic film. The effects of ion-implantation would be destroyed as soon as the film were immersed in the solution. However, the LPE GGG spacing layer is compatible with systems which are hard-bubble proofed by use of a second magnetic garnet film as a capping layer.

8. REPRODUCIBILITY AND ECONOMICS OF LPE GROWTH

Factors Influencing Reproducibility

There are a number of factors which must be considered when discussing the reproducibility of the LPE process. Perhaps the most important of these is the changing liquidus temperature as solute is removed from solution by film growth. For the systems studied here, the liquidus temperature decreases about 30°C per gram of garnet removed. Thus, at a constant growth temperature, the degree of supercooling becomes less as each film is grown. This, of course, affects the growth rate and, thereby, the concentration of Ga in the film and also the growth-induced anisotropy.

The effects of solute removal by film growth are partially offset by loss of PbO by evaporation. Rate of PbO evaporation depends upon growth and homogenization temperature, surface area of solution exposed, and the geometry and arrangement of baffles in the furnace.

In general, the growth of a series of films with nearly the same properties requires an adjustment of growth temperature and growth time between each run. Several additional factors must be considered when making the proper adjustment. These involve the dependence on growth temperature and/or growth rate of the following phenomena:

(1) Distribution coefficient of Ga

(2) Distribution coefficients of rare-earth ions

(3) Distribution of Ga ions on tetrahedral and octahedral sites

(4) Growth induced anisotropy

(5) Pb incorporation in the film

The precise adjustment to be made is determined empirically and is peculiar to the particular situation.

The following general observations are of help in making the adjustment.

(1) The distribution coefficient of Ga increases with temperature but tends toward unity with increasing growth rate and increasing Ga concentration. The range of Ga concentration in solution which is usually empolyed is so small that the dependence of the distribution coefficient on Ga concentration is not important generally.

(2) The distribution coefficients of the rare-earth ions depend primarily on the relative size of the ions in solution and are not strong functions of growth conditions. They do, however, tend toward unity as growth rate is increased.

(3) The preferential occupation of tetrahedral sites by Ga ions decreases as Ga concentration increases.

(4) The magnitude of the growth-induced anisotropy decreases with increasing film growth temperature.

(5) The incorporation of Pb increases with increasing growth rate but decreases with increasing growth temperature.

Experimental

The run-to-run reproducibility of the LPE growth process was studied by growing 10 films from each of two solutions. The control scheme adopted depended on the closest cooperation between the film grower and the characterization unit. A running tally was made of solute removal by weighing the sample before and after film growth. Film thickness, collapse field, characteristic length, and magnetization were immediately determined. These properties were compared to those of previously grown films and the results dictated the adjustments of growth temperature and time to be made for the next run.

Results are listed in Tables 5a and 5b. In the first case (Table 5a) films of the nominal composition: $Eu_{0.50}Yb_{0.05}Y_{2.45}Fe_{3.75}Ga_{1.25}O_{12}$ were grown at 990-980°C from a solution contained in a 5.7 cm diameter crucible. The aim was to grow films about 6 μm thick with a collapse field of about 80 Oe. The reproducibility is considered excellent.

TABLE 5

REPRODUCIBILITY OF THE LPE GROWTH PROCESS

A. FILM COMPOSITION $Eu_{0.5}Yb_{0.05}Y_{2.45}Fe_{3.75}Ga_{1.25}O_{12}$

Sample No.	Thickness (μm)	Saturation Magnetization (gauss)	Collapse Field (Oe)	Material Length (μm)
34572D	7.89	139	77	0.749
34572E	6.26	151	78	0.707
34572F	6.18	149	76	0.785
34572G	6.12	147	74	0.741
34572H	6.82	152	81	0.702
34571I	7.42	157	85	0.742
34572J	5.92	146	73	0.728
34572M	6.73	153	81	0.720
34572N	6.80	156	85	0.686
34572O	6.37	149	79	0.713
Average	6.65	150	79	0.720
Percent Average Deviation	7.2	2.7	3.8	2.1

B. FILM COMPOSITION $Eu_{0.4}Yb_{0.1}Y_{2.5}Fe_{3.8}Ga_{1.2}O_{12}$

34580K	7.21	154	84	0.721
34580L	4.52	135	55	0.822
34580M	5.21	137	60	0.828
34580N	6.66	160	85	0.692
34580O	5.13	148	69	0.743
34580P	5.62	148	71	0.769
34580Q	6.59	148	74	0.823
34580R	5.82	159	81	0.675
34580S	5.13	135	60	0.795
34580T	4.75	150	66	0.755
Average	5.66	147	70	0.762
Percent Average Deviation	12.8	4.9	11.4	5.9

The rate loss of PbO during the growth of the films listed in Table 5a was considered excessive. Therefore, lower growth temperatures (915-905°C) and a smaller crucible (4.2 cm) were used for the films listed in Table 5b in an effort to reduce the rate loss of PbO. In this case the nominal composition of the film is $Eu_{0.4}Yb_{0.1}Y_{2.5}Fe_{3.8}Ga_{1.2}O_{12}$. Again, a thickness of about 6 μm and a collapse field of about 80 Oe was the aim. Loss of PbO during this series of runs was significant but not as great as at the higher gorwth temperature.

The run-to-run reproducibility of this series is not quite as good as that listed in Table 5a. This is primarily due to the lack of experience of the film growers at such low growth temperatures. However, the reproducibility is considered satisfactory for the present stage of development of the LPE process.

Costs

Some insight into the economics of the LPE process can be gained by considering the costs of materials and effort involved in growing a 6 μm film of $Eu_{0.4}Yb_{0.1}Y_{2.5}Fe_{3.8}Ga_{1.2}O_{12}$ on a 2.54 cm diameter wafer of GGG. The composition and costs of a solution with a volume compatible with the substrate diameter is given in Table 6. The cost of materials given in the table are based on recent catalog prices of a reliable supplier of high quality materials. The prices refer to research quantities and, thus, are probably representative of the upper limit of the materials costs.

TABLE 6

COST OF LPE SOLUTION

Compound	Weight,g	Cost
PbO	500.0	$112.00
B_2O_3	10.0	3.30
Eu_3O_3	.67	2.77
Y_2O_3	2.69	0.67
Yb_2O_3	0.19	0.16
Fe_2O_3	30.08	9.92
Ga_2O_3	4.80	6.48
Total Cost		$135.30

It appears reasonable to assume that 1000 films could be grown before the solution is discarded because of crucible attack or impurity build up. Of course, this implies that "make-up" additions of the oxides are made at appropriate intervals. Since each film removes about 0.035 g of garnet from solution, a total of 35 g of garnet constituents would need to be added during the useful lifetime of the melt. If no PbO were lost by evaporation, the cost of the make-up additions is estimated at about $28,00, bringing the total cost of the materials to about $163. Therefore the materials cost per film is about $0.16 to $0.17. If all the PbO were lost by evaporation, the replenishment cost would be $140., bringing the total cost of the materials to about $275. The upper limit for materials costs per film would then be about $0.30.

At present, films are grown one-at-atime. Experience at Monsanto indicates that about 1.5 hours of skilled technician time is required to clean and mount a substrate, grow an expitaxial film, clean and dismount, and perform the necessary characterization. Therefore, a cost of about $10.00 appears reasonable. Since there appears to be no inherent reason why multiple film-growth cannot be accomplished, this labor cost probably is the maximum.

Based on the above considerations it appears to cost about $10.00 to grow an epitaxial garnet film on a 2.54 cm substrate. This cost will not be increased significantly if larger substrates are used because of the small material costs. On the other hand, costs can be reduced substantially if multiple film growth is undertaken.

To the above costs must be added additional materials costs, depreciation, overhead and other miscellaneous items which are more difficult to assess. One major item is the costs of the substrate. Experience at Monsanto indicates that a substrate with one side prepared for epitaxial growth can be produced at a cost of about $30.00. This includes the cost of a crystal, and slicing, lapping and polishing costs. Another item to be considered is the cost of platinum. The high purity platinum crucibles required for LPE are attacked by the $PbO-B_2O_3$ solvent and have to be discarded eventually. In this respect, it should be pointed at that additions of V_2O_5 to the solution have been found (ref. 33) to reduce crucible attack by the solvent. In any event, a substantial portion of the platinum value can be recovered by resale to the crucible manufacturer. Therefore, the platinum costs are not expected to add significantly to the costs per film discussed above.

The apparatus and facilities required for LPE growth of garnet films are relatively simple. The essential features of a dipping station are illustrated in Figure 3. Such a station should be contained in a laminar flow hood to insure clean conditions.

In fact, all steps of the LPE process (cleaning, mounting, etc.) should be done under dust-free conditions. Depreciation and maintenance costs might then be compared with the operation of a suitably equipped Class 100 clean room facility for the production of semiconductor materials.

Finally, the cost of a "usable" film will, of course, depend on the yield factor. Yields are determined by acceptable thickness uniformity, defect density and reproducible magnetic properties. Experience at Monsanto indicates that films with thickness variations less than 1% can be grown at better than 90% yield.

If solution compositions are properly adjusted, the LPE process, per se, is not a source of defects. Defects arise from substrate imperfections and from air borne dust and contaminants. With careful handling of the high quality substrate now available, films with defect free areas of at least 1 cm^2 can be grown at 70-80% yields.

The run-to-run reproducibility of magnetic properties is demonstrated in Table 5. In addition, the magnetic properties of films exhibiting growth induced anisotropy can be adjusted by relatively simple post-growth heat-treatment. Although such treatment may add to the cost of an individual film, it may improve overall yield significantly.

In summary, experience indicates that high yields might be expected. If such is true, then, based on these considerations, LPE appears as an attractive commercial process.

Conclusions

The run-to-run reproducibility demonstrated here and the economic considerations discussed above clearly indicate that the LPE dipping process is commercially viable. Remarkable progress has been made in the relatively short time the process has been used to grow magnetic garnet bubble films. It is reasonable to expect that additional progress will be made in the future. It is believed that nearly all workers in this field are now using LPE exclusively to grow bubble films and this situation is expected to continue.

9. COMPARISON OF LIQUID PHASE EPITAXY AND CHEMICAL VAPOR DEPOSITION

High quality uniaxial magnetic garnet films have been grown by both liquid phase epitaxy (LPE) and by chemical vapor deposition (CVD) in a number of laboratories. At present, LPE is the

most widely used growth process. Monsanto has investigated both LPE and CVD (on other programs) and recognizes certain advantages and disadvantages peculiar to each. The pertinent factors for each technique are discussed in detail below.

Advantages of LPE

(1) Simple:

The composition of the deposited layer depends on the composition of the solution, on deposition temperature and on growth rate. These factors can be controlled simply and easily, the first by accurate weighing of components, the second by proper design of furnace and temperature controllers and the third by control of supercooling and/or rotation rate.

(2) Adaptable to complex garnet compositions:

A wide variety of mixed and substituted garnets have been grown from solution and there appears to be no limit to the type or complexity of the magnetic garnet film which can be grown by LPE (provided, of course, the garnet of a particular rare earth ion can exist). Thus, it will be relatively easy to adapt the LPE manufacturing processes to grow new garnet compositions having improved thermal and dynamic properties as these are developed.

(3) Both growth-and strain-induced anisotropies possible:

Films which exhibit either strain-induced or growth-induced magnetic anisotropy can be grown by LPE. Since there is emerging a preference for growth-induced anisotropy, this must be considered a telling advantage in fabor of LPE, It allows a more direct comparison of the modes of uniaxiality and, also allows any garnet composition to be produced irrespective of anisotropy type.

(4) Conserves materials:

LPE is highly conservative of materials. Under proper conditions, there is no garnet deposit except on the substrate. The solvent can then be used for long periods merely by replenishing the garnet components. This is an important economic consideration for any potential commercial process.

(5) Fast fabrication:

The growth rate of LPE films depends on deposition temperature, the extent to which the solution is supersaturated and rotation rate. Growth rates of 1 μm/min are achieved easily. Thus, only 5-10 min are required to deposit films of the desired thickness. Such growth rates permit the growth of a large number of films in a short time.

(6) Feasibility of post-growth tailoring of anisotropy:

It is possible to tailor the anisotropy of "as grown" LPE magnetic-garnet layers. Growth induced anisotropy, which for some compositions is too large, can be annealed downward resulting in smaller bubble diameters. This may prove to be a convenient technique for matching bubble dilms to propagation circuits in a production environment.

Disadvantages of LPE

(1) Incorporates Pb:

Although high purity compounds can be used in LPE, all garnet films grown from PbO based solvents will contain some Pb. The incorporation of Pb in the garnet structure varies with growth temperature and growth rate and can be as high as a few weight percent. Under proper conditions, however, the Pb incorporation will be less than 1 wt %. Although impurities in the magnetic garnet film are not desirable, Pb contamination at this low level does not seem seriously to effect the magnetic properties of the garnet.

(2) Flux scars:

Invariably a small droplet of solution will cling to the substrate/epitaxial layer when it is withdrawn from the solution. This results in a spot, or scare, of non-uniform or dendritic growth which reduces the usable area of the magnetic film.

Advantages of CVD

(1) Lower impurity incorporation:

Volatile impurities in starting materials are the source of contamination of CVD films. Since all the starting materials used in CVD are commercially available in 99.99% or better purity, the chemical purity of CVD films can be quite high.

Disadvantages of CVD

(1) Strain-induced anisotropy:

Deposition temperatures approaching 1200°C are required to achieve smooth epitaxial films of the magnetic garnets. It is doubtful whether the pair-ordering required for growth-induced anisotropy can be achieved at such temperatures. Indeed, 1200°C is sufficient to anneal out the anisotropy in most garnets which exhibit growth-induced magnetic anisotropy.

(2) Complicated:

The apparatus used for CVD of magnetic garnets is relatively complex -- requiring a multi-zone furnace with individual zone temperature controllers plus rather elaborate gas flow control systems.

(3) Reproducibility difficult:

In the CVD process, appropriate metal halides are evaporated into a carrier gas stream. The mass transport rates depend not only on temperature and carrier gas flow rate, but also on the exposed surface area of the evaporating material. Thus, the size and shape of the halide containers also effect mass transport rates. In such systems it is difficult to maintain a constant evaporation rate as the level of the material drops in the container and the reproducibility of the process suffers. This problem becomes more acute for complex garnet films containing two or more rare-earths and the number of evaporation rates which must be controlled is increased.

(4) Limited post-growth tailoring of anisotropy:

There is no technique for altering the anisotropy of "as-grown" CVD layers subsequent to growth.

Summary of Epitaxial Technique Comparison

Both CVD and LPE lend themselves to batch processing. It should be possible to scale either method to handle a number of substrates at a time. However, it is our opinion that of the two processes LPE is clearly to be fovored. This is dramatically evident in Table 7 which summarizes the advantages and disadvantages of the two methods. The low cost and adaptability of LPE are most desirable from a commercial viewpoint, enabling the manufacturer to change his formulations with a minimum of trouble to keep

Table 7

COMPARISON OF LPE AND CVD FOR BUBBLE-GARNET FILMS

LPE Advantages	CVD Advantages
1. Simple 2. Adaptable to complex garnet compositions 3. Both growth- and strain-induced anisotropies achievable 4. Conserves materials 5. Fast fabrication 6. Post-growth anisotropy tailoring possible	1. Lower impurity incorporation
LPE Disadvantages	**CVD Disadvantages**
1. Incorporates Pb 2. Flux scars occur	1. Limited to strain-induced anisotropy 2. Complicated 3. Reproducibility difficult to achieve 4. Post-growth anisotropy tailoring limited

abreast with developments in magnetic bubble device technology. In addition, the reproducibility of LPE has been demonstrated. The almost exclusive use of LPE by workers in the field of bubble materials support this conclusion.

10. CONCLUSIONS AND RECOMMENDATIONS

The results and conclusions of this program have been discussed in detail in the various sections of this report. The major conclusions are briefly restated here:

(1) The properties of the Gd-Y mixed garnets are not suitable for exploitation in practical magnetic bubble devices.

(2) Garnet systems which exhibit growth-induced, rather than stress-induced, uniaxial anisotropy are preferred for bubble device application.

(3) The Eu-Yb-Y system appears to be an attractive candidate material for bubble device applications.

(4) It is feasible to deposit GGG spacing layers on magnetic films by LPE.

(5) Compared to CVD, LPE is the more attractive technique from which to develop large scale production of magnetic garnet films.

On the basis of the data presented in this report it is recommended that NASA consider the Eu-Yb-Y garnet system a serious candidate as the host magnetic material for eventual NASA bubble memory systems. Compositions have been identified which have nearly optimal properties, and the LPE growth processes have been sufficiently refined to demonstrate the potential availability of an adequate and reproducible supply of bubble material at reasonable economy.

REFERENCES

1. R. C. Linares, R. B. McGraw and J. B. Schroeder, "Growth and Properties of Yttrium Iron Garnet Single-Crystal Films", J. Appl. Phys., 31, 2884 (1965).

2. R. C. Linares, "Epitaxial Growth of Narrow Linewidth Yttrium Iron Garnet Films", J. Cryst. Growth, 34, 443, (1968).

3. L. K. Shick, J. W. Nielsen, A. H. Bobeck, A. J. Kurtzig, P. C. Michaelis and J. P. Reekstin, "Liquid Phase Epitaxial Growth of Uniaxial Garnet Films: Circuit Deposition and Bubble Propogation", Appl. Phys. Letters, 18, 89 (1971).

4. H. J. Levinstein, S. Licht, R. W. Landorf and S. L. Blank, "Growth of High-Quality Thin Films from super-cooled Melts", Appl. Phys. Letters, 19, 486, (1971).

5. see, for example, R. Hiskes and R. A. Burmeister, "Properties of Rare Earth Iron Garnets Grown in BaO-Based and PbO-Based Solvents", AIP Conference Proceedings, No. 10, 304 (1973).

6. E. A. Giess, J. D. Kuptsis and E. A. D. White, "Liquid Phase Epitaxial Growth of Magnetic Garnet Films by Isothermal Dipping in a Horizontal Plane with Axial Rotation", J. Cryst. Growth, 16, 36, (1972).

7. R. Ghez and E. A. Giess, "Liquid Phase Epitaxial Growth Kinetics of Magnetic Garnet Films Grown by Isothermal Dipping with Axial Rotation", Mat. Res. Bull., 8, 31 (1973).

8. S. L. Blank, B. S. Hewitt, L. K. Shick and J. W. Nielsen, "Kinetics of LPE Growth and Its Influence on Magnetic Properties", AIP Conference Proceedings, No. 10, 256 (1973).

9. R. W. Shaw, R. M. Sandfort and J. W. Moody, Magnetic Bubble Materials: Initial Characterization Report, March, 1972, Tech. Req. No. 1533, ARPA Order 1999, Contract No. DAAHO1-72-C-0490.

10. R. W. Shaw, R. M. Sandfort and J. W. Moody, Magnetic Bubble Materials: Characterization Techniques Study Report, July, 1972, Tech. Req. No. 1533, ARPA Order 1999, Contract No. DAAHO1-72-C-0490.

11. J. W. Moody, R. M. Sandfort and R. W. Shaw, Magnetic Bubble Materials: Final Report, August, 1972, ARPA Order 1999, Contract No. DAAHO1-72-C-0490.

12. D. C. Fowlis and J. A. Copeland, "Rapid Method for Determining the Magnetization and Intrinsic Length of Magnetic Bubble Domain Materials", AIP Conference Proceedings, No. 5, 240 (1971).

13. R. W. Shaw, D. E. Hill, R. M. Sandfort, and J. W. Moody, "Determination of Magnetic Bubble Film Parameters from Strip Domain Measurements", J. Appl. Phys., 44, 2346 (1973).

14. A. A. Thiele, "Theory of the Static Stability of Cylindrical Domains in Uniaxial Platelets", J. Apple. Phys., 41, 1139 (1970).

15. P. W. Shumate, Jr., D. H. Smith and B. F. Hagedorn, "The Temperature Dependence of the Anisotropy and Coercivity in Epitaxial Films of Mixed Rare-Earth Iron Garnets", J. Appl. Phys., 44, 449 (1973).

16. P. W. Shumate, Jr., "Extension of the Analysis for An Optical Magnetometer to Include Cubic Anisotropy in Detail", J. Appl. Phys., 44, 3323 (1973).

17. R. M. Josephs, "Characterization of the Magnetic Behavior of Bubble Domains", AIP Conference Proceedings, No. 10, 286 (1973).

18. J. A. Seitchik, W. D. Doyle and G. K. Goldberg, "Simple Method of Measuring Mobility in Cylindrical Domain Materials", J. Appl. Phys., 42, 1272 (1972).

19. B. E. Argyle and A. P. Malozemoff, "Experimental Study of Domain Wall Response to Sinusoidal and Pulsed Fields", AIP Conference Proceedings, No. 5, 115 (1972).

20. D. C. Cronemeyer, E. A. Giess, E. Klokholm, B. E. Argyle and T. S. Plaskett, "Annealing of LPE Garnet Films", AIP Conference Proceedings, No. 5, 115 (1972).

21. W. T. Stacy, M. M. Janssen, J. M. Robertson and M. J. G. van Hout, "Dependence of the Uniaxial Magnetic Anisotropy on the Misfit Strain in Gd, Ga:YIG LPE Films", AIP Conference Proceedings, No. 10, 314 (1973).

22. G. P. Vella-Coleiro, D. H. Smith and L. G. Van Uitert, "Resonant Motion of Domain Walls in Yttrium Gadolinium Iron Garnets", J. Appl. Phys., 43, 2428 (1972).

23. G. P. Vella-Coleiro, D. H. Smith and L. G. Van Uitert, "Damping of Domain Wall Motion in Rare Earth Iron Garnets", Appl. Phys. Letters, 21, 36 (1972).

24. see, for example, S. Chikazumi, Physics of Magnetism, 394, John Wiley, New York (1964).

25. S. Geller, "Crystal Chemistry of the Garnets", Z. Krist., 125, 1 (1967).

26. E. A. Giess, B. E. Argyle, B. A. Calhoun, L. C. Cronemeyer, E. Klokholm, L. R. McGuire and T. S. Plaskett, "Rare Earth Yttrium Iron-Gallium Epitaxial Films for Magnetic Bubble Domain Applications", Mat. Res. Bull., 6, 1141 (1971).

27. T. S. Plaskett, E. Klokholm, D. C. Cronemeyer, B. E. Argyle, V. Sadagopan and P. Chaudhari, "The LPE Growth and Properties of $(Gd\text{-}Y)_3(Ga\text{-}Fe)_5O_{12}$ Films for Bubble Domain Memory Applications", paper No. 8 141st. National Meeting, Elec. Chem. Soc., Houston (1972).

28. W. A. Bonner, J. E. Geusic, D. H. Smith, F. C. Rossol, L. G. Van Uitert and G. P. Vella-Coleiro, "Characteristics of Temperature-Stable Eu-Based Garnet Films for Magnetic Bubble Applications", J. Appl. Phys., 43, 3226 (1972).

29. G. P. Vella-Coleiro, "Domain Wall Mobility in Epitaxial Garnet Films", AIP Conference Proceedings, No. 10, 424 (1973).

30. E. Schloemann, "Light and Heavy Domain Walls in Bubble Films", AIP Conference Proceedings, No. 10, 478 (1973).

31. S. Geller, G. P. Espinosa and P. B. Crandall, "Thermal Expansion of Yttrium and Gadolinium Iron, Gallium and Aluminum Garnets", J. Appl. Cryst., 86 (1969).

32. S. Geller, G. P. Espinosa, L. D. Fullmer and P. B. Crandall, "Thermal Expansion of Some Garnets", Mat. Res. Bull., 7, 1219 (1972).

33. B. S. Hewitt, R. D. Pierce, S. L. Blank and S. Knight, "Technique for Controlling the Properties of Magnetic Garnet Films", Intermag Conference, Washington D. C., 1973.

APPENDIX

Substrate Preparation

If the proper solution composition and growth conditions are employed, the LPE process, per se, does not give rise to magnetic pinning defects in the epitaxial film. In addition core-free substrates with less than 5 dislocations/cm^2 can be grown and, indeed, are now commercially available. Therefore, the major sources of defects in magnetic garnet films are inadequate polishing procedures and improper housekeeping habits. Lapping, polishing and cleaning procedures that produce an excellent, defect-free surface for epitaxial growth have been developed at Monsanto. Since these procedures are so important to the perfection of the epitaxial film, they are described in detail here.

Wafers of nominal 0.05 cm thickness are sliced from an oriented GGG crystal with a diamond impregnated OD saw. The wafers are cleaned and cemented onto a stainless steel lapping block using a minimum of carnauba wax. The wafers are then lapped to the same thickness on a Lapmaster machine equipped with a cast iron lapping plate; 3 μm Al_2O_3 suspended in a mixture of deionized water and glycerine is used as the abrasive.

The wafers are then demounted and throughly cleaned as described below. Since at Monsanto only one side of the wafer is prepared for epitaxial growth, the wafers are now etched for 5 min in orthophosphoric acid. This serves to release strain introduced by lapping and prevents "bowing' of the wafer when the second side is finished.

The wafers are remounted on the stainless steel lapping block. Again a minimum of carnauba wax is used to cement the wafers and all excess wax is carefully removed from the wafers and lapping block. The wafers are again lapped on the Lapmaster, using 3 μm Al_2O_3, until at least 0.005 cm of material is removed. The wafers and block are then scrubbed with warm soapy water and nylon brush, soaked in warm soapy water in an ultrasonic cleaner and finally rinsed in deionized water.

Finally, at least 0.003 cm of surface is removed on a Syton flooded Corfam lap. The Syton is used full strength. The final thickness of the wafer is about 0.04 cm.

After demounting, the wafers are rinsed three times in boiling trichloroethylene, then once in boiling isopropyl alcohol and dried in a stream of filtered nitrogen. To ensure that all traces of Syton have been removed, the wafers are then soaked for 10 sec in concentrated HF. After rinsing in deionized water and drying in hot isopropyl alcohol the wafers are mounted in a Teflon rack and given a final cleaning:

1. 5 minute soak in each of two beakers of warm (50°C) H_2SO_4

2. 3 rinses in deionized H_2O

3. 1 rinse in hot isopropyl alcohol in an ultrasonic cleaner

4. 1 rinse in hot isopropyl alcohol

5. Dried in a steam of filtered N_2

(The sulfuric acid and solvents used in the cleaning procedure are Transist AR grade obtained from Mallinckrodt Chemical Works). Good housekeeping habits and cleanliness cannot be over-stressed in the polishing and cleaning procedures.

These procedures have been found to produce excellent surfaces for the growth of epitaxial garnet films. Etching in hot orthophosphoric acid at 160-170°C reveals no scratches or residual work damage. However, the Syton polishing does result in considerable rounding of the edges of the wafers. Other polishing methods have been investigated in an effort to preserve the flatness of the wafers. These have included polishing with diamond on a tin lap, and with Syton on both a Teflon and polyurethane lap. Although flatness was preserved by these methods, the resulting surfaces were not free of work damage.

Properties of Samples Supplied NASA

Sample Number	h	ℓ	$4\pi M_s$	σ_w	H_c	H_A	H_{S-B}	d_{S-B}	H_o	d_o	T_N	$\frac{1}{\ell}\frac{d\ell}{dT}$	$\frac{1}{M}\frac{dM}{dT}$	μ
EuYYb-21	6.37	0.71	149	0.12	0.25	1150	57	8	78	3	117	0.0054	0.0028	1000
EuYYb-22	7.86	0.54	177	0.14	0.25	1150	77	8	108	3	122	"	"	"
EuYYb-23	6.39	0.69	153	0.13	0.20	1100	56	8	80	2	118	"	"	"
EuYYb-24	5.88	0.70	148	0.12	0.025	1200	55	7	74	3	116	"	"	"
EuYYb-25	7.18	0.67	155	0.13	0.30	1200	66	8	86	3	118	"	"	"
EuYYb-26	4.18	0.78	139	0.12	0.25	1150	37	9	56	2	116	"	"	"
EuYYb-27	6.66	0.69	160	0.11	0.40	1200	61	9	85	3	125	0.0040	0.0025	"
EuYYb-28	5.62	0.77	148	0.13	0.25	1200	48	9	70	4	124	"	"	"
EuYYb-29	5.13	0.80	135	0.11	0.55	1350	42	9	60	3	125	"	"	"
EuYYb-30	4.75	0.76	148	0.13	0.45	1450	43	9	66	3	126	"	"	"
EuYYb-31	5.18	0.78	148	0.14	0.50	1450	47	9	68	4	126	"	"	"
EuYYb-32	4.47	0.82	123	0.10	0.34	1200	34	9	50	2	113	0.0065	0.0040	"

Composition	Sample Numbers
$Eu_{0.5}Yb_{0.05}Y_{2.45}Fe_{3.8}Ga_{1.2}O_{12}$	EuYYb-21 EuYYb-22 EuYYb-23 EuYYb-24 EuYYb-25 EuYYb-26
$Eu_{0.5}Yb_{0.1}Y_{2.5}Fe_{3.3}Ga_{1.2}O_{12}$	EuYYb-27 EuYYb-28 EuYYb-29 EuYYb-30 EuYYb-31
$Eu_{0.4}Yb_{0.2}Y_{2.4}Fe_{3.7}Ga_{1.2}O_{12}$	EuYYb-32

LEGEND

h	Thickness, μm
ℓ	Characteristic Length, μm
$4\pi M_s$	Saturation Magnetization, gauss
d_{S-B}	Bubble diameter at H_{S-B}, μm
H_o	Bubble collapse field, Oe
d_o	Bubble diameter at H_o, μm
σ_w	Domain wall energy/unit area, ergs/cm^2
H_c	Coercivity, Oe
H_A	Anisotropy, Oe
μ	Mobility, cm/sec/Oe
T_N	Neel Temperature, °C
H_{S-B}	Strip to Bubble Transition filed, Oe
$\frac{1}{\ell}\frac{d\ell}{dT}$	Temperature Coefficient of Characteristic Length, K^{-1}
$\frac{1}{M}\frac{dM}{dT}$	Temperature Coefficient of Magnetization, K^{-1}

U.S. GOVERNMENT PRINTING OFFICE: 1974—737-769/100 REGION NO. 3-11

NATIONAL AERONAUTICS AND SPACE ADMINISTRATION
WASHINGTON, D.C. 20546

OFFICIAL BUSINESS
PENALTY FOR PRIVATE USE $300

SPECIAL FOURTH-CLASS RATE
BOOK

POSTAGE AND FEES PAID
NATIONAL AERONAUTICS AND
SPACE ADMINISTRATION
451

POSTMASTER: If Undeliverable (Section 158 Postal Manual) Do Not Return

"The aeronautical and space activities of the United States shall be conducted so as to contribute . . . to the expansion of human knowledge of phenomena in the atmosphere and space. The Administration shall provide for the widest practicable and appropriate dissemination of information concerning its activities and the results thereof."

—NATIONAL AERONAUTICS AND SPACE ACT OF 1958

NASA SCIENTIFIC AND TECHNICAL PUBLICATIONS

TECHNICAL REPORTS: Scientific and technical information considered important, complete, and a lasting contribution to existing knowledge.

TECHNICAL NOTES: Information less broad in scope but nevertheless of importance as a contribution to existing knowledge.

TECHNICAL MEMORANDUMS: Information receiving limited distribution because of preliminary data, security classification, or other reasons. Also includes conference proceedings with either limited or unlimited distribution.

CONTRACTOR REPORTS: Scientific and technical information generated under a NASA contract or grant and considered an important contribution to existing knowledge.

TECHNICAL TRANSLATIONS: Information published in a foreign language considered to merit NASA distribution in English.

SPECIAL PUBLICATIONS: Information derived from or of value to NASA activities. Publications include final reports of major projects, monographs, data compilations, handbooks, sourcebooks, and special bibliographies.

TECHNOLOGY UTILIZATION PUBLICATIONS: Information on technology used by NASA that may be of particular interest in commercial and other non-aerospace applications. Publications include Tech Briefs, Technology Utilization Reports and Technology Surveys.

Details on the availability of these publications may be obtained from:

SCIENTIFIC AND TECHNICAL INFORMATION OFFICE

NATIONAL AERONAUTICS AND SPACE ADMINISTRATION

Washington, D.C. 20546